

# DYSON-SCHWINGER EQUATIONS IN MINIMAL SUBTRACTION

PAUL-HERMANN BALDUF

**ABSTRACT.** We compare the solutions of one-scale Dyson-Schwinger equations in the Minimal subtraction (MS) scheme to the solutions in kinematic (MOM) renormalization schemes. We establish that the MS-solution can be interpreted as a MOM-solution, but with a shifted renormalization point, where the shift itself is a function of the coupling. We derive relations between this shift and various renormalization group functions and counter terms in perturbation theory.

As concrete examples, we examine three different one-scale Dyson-Schwinger equations, one based on the D=4 multiedge graph, one for the D=6 multiedge graph and one mathematical toy model. For each of the integral kernels, we examine both the linear and nine different non-linear Dyson-Schwinger equations. For the linear cases, we empirically find exact functional forms of the shift between MOM and MS renormalization points. For the non-linear DSEs, the results for the shift suggest a factorially divergent power series. We determine the leading asymptotic growth parameters and find them in agreement with the ones of the anomalous dimension. Finally, we present a tentative exact non-perturbative solution to one of the non-linear DSEs of the toy model.

## 1. INTRODUCTION

**1.1. Motivation.** So far, the systematic Hopf-algebraic treatment [30, 29, 40, 7, 6, 5, 28, 26] of Dyson-Schwinger equations (DSEs) [24, 37] has relied on kinematic renormalization schemes, called MOM hereafter. The solution of a DSE is the renormalized Green function  $G(p^2)$ . MOM schemes assign a value to the renormalized Green function  $G(p^2)$  at one particular momentum  $p^2 = \mu^2$ , and thereby have a transparent interpretation as boundary condition for the DSE. For a single (non-coupled) DSE, the only remaining unknown object is the anomalous dimension  $\gamma(\alpha)$  as a function of the renormalized coupling  $\alpha$ . If MOM-conditions are used systematically, explicit regularization of divergent integrals is not necessary [30, 29] and one only deals with finite quantities at all stages. In fact,  $\gamma(\alpha)$  can be computed from a differential equation without any divergent integral. The earlier works [22, 23] do regulate the integrals explicitly using dimensional regularization [2, 8], but they use MOM renormalization conditions nonetheless.

On the other hand, many perturbative computations in quantum field theory use the combination of dimensional regularization and Minimal Subtraction (MS) renormalization conditions. In this scheme, all singular terms in the regulator  $\epsilon$  are subtracted, but the resulting amplitude does not respect any particular kinematic boundary condition. The MS-solution of a DSE can only be found by explicitly regulating and renormalizing the divergent integrals at each loop order.

At the same time, different renormalization schemes should not lead to different physical outcomes, therefore, there ought to be *some* particular momentum  $\hat{\mu}$  such that Minimal Subtraction agrees with kinematic renormalization using that very reference momentum  $\hat{\mu}$ . Finding this correspondence is of practical relevance since the perturbative solution is typically only known to a few orders. In that case, the truncated MS-renormalized results are truly different from the MOM ones and a priori only valid around their respective renormalization points [16]. Knowing the physical value of the MS-renormalization point  $\hat{\mu}$  is then crucial for the validity range of the truncated Green function. Furthermore, renormalization group functions differ between both schemes. In MS, but

---

The author thanks Dirk Kreimer for encouragement and several discussions, and Gerald Dunne for comments and suggestions on the draft.

presumably not in MOM, the beta function is expected to be dominated by subdivergence-free diagrams [34]. A better understanding of the relation between MOM and MS can help to translate such conjectures to the other scheme and subsequently attack them with a different set of tools.

**1.2. Content.** The present paper begins in section 2 with a pedagogic discussion of  $Z$ -factors and renormalization group equations in both MOM and MS and their various relations and identities. In section 3, we establish that, in the physical limit  $\epsilon \rightarrow 0$ , the Green function in MS can be interpreted as a MOM Green function with shifted renormalization point. We derive several ways to compute this shift.

In the remainder, we analyse propagator-type Dyson-Schwinger equations based on three different primitive integral kernels. The first one is the 4-dimensional bubble (=1-loop-multiedge) graph appearing e.g. in the fermion propagator in Yukawa theory. The second one is the same graph in 6 dimensions, contributing to the  $\phi^3$ -propagator, and the third is a mathematical toy model which has occasionally been used to study renormalization. In all three cases, we consider the recursive insertion of the Green function into only one place in the kernel graph.

First, we insert the Green function itself, which amounts to a linear DSE known as the rainbow approximation. In section 4, the algorithm for linear DSEs is developed for the case of the 4-dimensional bubble integral. Subsequently, this is applied to the  $D = 6$  case in section 5 and to the toy model in section 6.

Secondly, we insert the Green function raised to a power  $\in \{-4, \dots, +6\}$ , producing non-linear DSEs. In section 7, the algorithm for non-linear DSEs is explained and used for the 4-dimensional model. The last sections 8 and 9 contain the results for the non-linear DSEs for the two remaining models,  $D = 6$  and the toy model. Section 10 is a summary of the results.

## 2. THEORETICAL BACKGROUND

**2.1. Unrenormalized Dyson-Schwinger equation.** We consider DSEs of the form

$$(2.1) \quad G_0(\alpha_0, x) = 1 + \alpha_0 \int dy K(x, y) Q(G_0(\alpha_0, y)) G_0(\alpha_0, y)$$

where  $G_0(\alpha_0, x)$  is the unrenormalized Green function and  $K(x, y)$  is an integral kernel, determined by a single primitive Feynman diagram. Restricting the Green function to depend on only one single external scale  $x$ , means that  $G_0(\alpha_0, x)$  represents a 1PI 2-point-function and  $K(x, y)$  stems from a propagator-type diagram. For a more general Green function, one needs to include also scale-less “angle” variables [14]. The variable  $x := p^2/\mu^2$  is the external momentum scaled to some fixed reference momentum  $\mu$ . In the literature, propagator-type DSEs are often written with a minus sign,  $G = 1 - \alpha \int \dots$ . We will use a plus for all DSEs considered in this work.

In the cases we consider, the invariant charge is a monomial of the Green function,

$$(2.2) \quad Q(G_0(\alpha_0, x)) = (G_0(\alpha_0, x))^s.$$

**2.2. Renormalization.** Carrying out renormalization on an integral- (rather than integrand-)level requires to regulate the divergent integrals. In dimensional regularization [2, 8], the space-time dimension is changed by a non-integer shift  $\epsilon$ , we choose  $D = 4 - 2\epsilon$  or  $D = 6 - 2\epsilon$ . The unrenormalized amplitude of a finite graph is then a Laurent series in the regularization parameter  $\epsilon$ .

We will only consider DSEs of multiplicatively renormalizable theories. This means that it is possible to eliminate all divergences at order  $m$  by two counter terms  $Z_G^{(m)}$  and  $Z_\alpha^{(m)}$ . They act as a rescaling of the Green function and the coupling constant according to

$$(2.3) \quad \alpha_0 = Z_\alpha(\alpha, \epsilon) \mu^{2\epsilon} \cdot \alpha, \quad G(\alpha, \epsilon, x) = Z_G(\alpha, \epsilon) \cdot G_0(Z_\alpha(\alpha, \epsilon) \alpha, \epsilon, x).$$

These  $Z$ -factors are themselves functions of the renormalized coupling  $\alpha$  and of the regularization parameter  $\epsilon$ .

Renormalization of the coupling constant is only necessary if the theory has a non-vanishing beta function or, equivalently, a running coupling. See [31] for a recent account. Eventually,  $Z_\alpha$  is given by the renormalization of the invariant charge  $Q$ . In the present case where there is only one Green function  $G(\alpha, x)$  which needs renormalization, the invariant charge eq. (2.2) leads to the identity

$$(2.4) \quad Z_\alpha(\alpha, \epsilon) = (Z_G(\alpha, \epsilon))^s.$$

The derivative of the renormalized coupling constant with respect to logarithmic momentum at the renormalization point is the beta function of the theory,

$$(2.5) \quad \beta(\alpha, \epsilon) := \mu^2 \frac{\partial}{\partial \mu^2} \ln \alpha(\alpha_0, \mu) + \epsilon = \frac{-\epsilon}{\alpha \frac{\partial}{\partial \alpha} \ln(\alpha \cdot Z_\alpha(\alpha, \epsilon))} + \epsilon$$

The anomalous dimension, on the other hand, is defined as the derivative of the renormalized Green function at the renormalization point,

$$(2.6) \quad \gamma(\alpha, \epsilon) := \mu^2 \frac{\partial}{\partial \mu^2} \ln G(\alpha, \epsilon) = (\beta(\alpha, \epsilon) - \epsilon) \alpha \frac{\partial}{\partial \alpha} \ln Z_G(\alpha, \epsilon).$$

Note that sometimes,  $\gamma$  is defined as the derivative of the inverse (i.e. connected, not 1PI) 2-point Green function, or as the derivative with respect to  $\mu$ . These definitions are equivalent up to overall signs and factors.

Conversely, the renormalization group functions  $\beta(\alpha, \epsilon)$  and  $\gamma(\alpha, \epsilon)$  uniquely determine the counter terms via

$$(2.7) \quad Z_\alpha(\alpha, \epsilon) = \exp \left( - \int_0^\alpha \frac{du}{u} \frac{\beta(u, \epsilon)}{\epsilon - \beta(u, \epsilon)} \right), \quad Z_G(\alpha, \epsilon) = \exp \left( - \int_0^\alpha \frac{du}{u} \frac{\gamma(u, \epsilon)}{\epsilon - \beta(u, \epsilon)} \right).$$

Such relations have long been known in the traditional formulation (“Gross-’t Hooft relations”) [1, 17, 25] as well as in the Hopf-algebraic formulation (“scattering type formula”) of quantum field theory [19],[20, Sec. 7].

It follows from the above definitions that the renormalized Green function  $G$  fulfils – even for  $\epsilon \neq 0$  and not only in MOM renormalization – the Callan-Symanzik equation [15, 39]

$$(2.8) \quad (\gamma(\alpha, \epsilon) + (\beta(\alpha, \epsilon) - \epsilon) \alpha \partial_\alpha) G(\alpha, \epsilon, x) = x \partial_x G(\alpha, \epsilon, x).$$

The renormalization group functions  $\beta, \gamma$  as well as the renormalized Green function are generally non-trivial functions of the regularisation parameter  $\epsilon$ . Assuming that the counter terms eq. (2.3) are chosen correctly, their limit  $\epsilon \rightarrow 0$  exists.

$$(2.9) \quad \beta(\alpha) := \lim_{\epsilon \rightarrow 0} \beta(\alpha, \epsilon), \quad \gamma(\alpha) := \lim_{\epsilon \rightarrow 0} \gamma(\alpha, \epsilon), \quad G(\alpha, x) := \lim_{\epsilon \rightarrow 0} G(\alpha, \epsilon, x).$$

This limit is usually implied when talking about the renormalized quantities. If the invariant charge has the form eq. (2.2) and consequently eq. (2.4) holds, then by eq. (2.7)

$$(2.10) \quad \beta(\alpha, \epsilon) = s \cdot \gamma(\alpha, \epsilon) \quad \Rightarrow \quad \beta(\alpha) = s \cdot \gamma(\alpha).$$

To directly compute the renormalization constants and renormalized solution from a DSE, one inserts eq. (2.1) into eq. (2.3) and uses eqs. (2.2) and (2.4) to obtain

$$(2.11) \quad \begin{aligned} G(\alpha, x) &= Z_G \left( 1 + Z_\alpha \alpha \int dy K(x, y) (G_0(Z_\alpha \alpha, y))^{s+1} \right) \\ &= Z_G + \alpha \int dy K(x, y) Q(G(\alpha, y)) G(\alpha, y). \end{aligned}$$

This equation can be solved iteratively by inserting the solution of order  $(m-1)$ ,  $G^{(m-1)}(\alpha, y)$ , into the right hand side to obtain the order- $m$ -solution  $G^{(m)}(\alpha, x)$ . We assume that no IR-divergences appear. The integrand is finite because it is a power of a renormalized Green function, therefore

the integral is only superficially divergent. The so-obtained divergence is of order  $\alpha^m$  and can be absorbed by a suitable summand in  $Z_G^{(m)}$ , producing a finite  $G^{(m)}(\alpha, x)$ .

**2.3. MOM scheme.** The counter terms introduced in eq. (2.3) are not unique. To fix them, one needs a renormalization condition. In the MOM scheme, this is done by fixing one particular momentum  $\delta \cdot \mu^2$ , where  $\delta \in \mathbb{R}$  and  $\mu$  is an arbitrary but fixed reference momentum. One then demands the renormalized Green function to take the value unity at that momentum. Introducing  $x := p^2/(\delta\mu^2)$ , the MOM renormalization condition is

$$(2.12) \quad G(\alpha, x = 1) = 1 \quad (\text{MOM scheme}).$$

This is achieved order by order in eq. (2.11) if one includes not only the pole term (in  $\epsilon$ ), but all finite parts of the amplitude into the counterterm  $Z^{(m)} = Z^{(m-1)} - \mathcal{R}[\dots]$ . The MOM-scheme operator  $\mathcal{R}$  projects the integral to a fixed scale  $x = 1$ .

Using eq. (2.10) and the limit eq. (2.9), the Callan-Symanzik equation eq. (2.8) becomes

$$(2.13) \quad \gamma(\alpha) \left( 1 + s\alpha \frac{\partial}{\partial \alpha} \right) G(\alpha, x) = x \frac{\partial}{\partial x} G(\alpha, x).$$

At the renormalization point  $x = 1$ , eqs. (2.12) and (2.13) lead to

$$(2.14) \quad \gamma(\alpha) = x \partial_x G(\alpha, x) \Big|_{x=1}.$$

**2.4. Expansion in logarithms.** The renormalized solution of a 1-scale DSE in MOM-renormalization with renormalization point  $x = 1$  can be expanded in logarithms according to

$$(2.15) \quad G(\alpha, x) = 1 + \sum_{k=1}^{\infty} \gamma_k(\alpha) (\ln x)^k.$$

From eq. (2.14) we identify the anomalous dimension  $\gamma_1(\alpha) = \gamma(\alpha)$ . The functions  $\gamma_{k>1}(\alpha)$  in eq. (2.15), with invariant charge eq. (2.2), can be computed from eq. (2.13) [30]:

$$(2.16) \quad \gamma(\alpha) (1 + s\alpha \partial_\alpha) \gamma_{k-1}(\alpha) = k \gamma_k(\alpha).$$

For a linear DSE, the exponent in the invariant charge eq. (2.2) is  $s = 0$ , and consequently one obtains  $\gamma_k(\alpha) = \frac{1}{k!} \gamma^k(\alpha)$ . This corresponds to a scaling solution of eq. (2.13),

$$(2.17) \quad G(\alpha, x) = x^{\gamma(\alpha)}.$$

The striking advantage of using MOM renormalization conditions for a Dyson-Schwinger equation is that the anomalous dimension  $\gamma(\alpha)$  is the only truly unknown function, and it itself can be computed from a non-linear ODE. This ODE is constructed by inserting the renormalization-group differential operator eq. (2.16) into the Mellin transform of the primitive kernel[30, 40]:

$$(2.18) \quad \frac{1}{-u \cdot M(u)} \Big|_{u \rightarrow -\gamma(1+s\alpha \partial_\alpha)} \gamma(\alpha) = \alpha.$$

See appendix A for the Mellin transforms of the kernels used in this paper. A linear DSE with  $s = 0$  reduces to the algebraic equation  $M(-\gamma(\alpha)) = \alpha^{-1}$  [29].

There is a second expansion of the renormalized Green function  $G(\alpha, x)$  in terms of logarithms, the leading-log expansion. It is a reordering of eq. (2.15) in powers of  $(\alpha \ln x)$ ,

$$(2.19) \quad G(\alpha, x) = 1 + \sum_{k=1}^{\infty} H_k(\alpha \ln x) \alpha^k.$$

The function  $H_1(z)$  is the leading-log contribution to the Green function, and  $H_k(z)$  represents the next-to<sup>k</sup> leading log part. These expansions have been studied recently [32, 21, 31], one of the results being that for a DSE eq. (2.11) with invariant charge eq. (2.2) where  $s \neq 0$  one has [31]

$$(2.20) \quad H_1(z) = (1 + sg_1z)^{-\frac{1}{s}}, \quad H_2(z) = \frac{(1 + sg_1z)^{-\frac{1}{s}-1}}{-sg_1} g_2 \ln(1 + sg_1z)$$

$$H_3(z) = \frac{(1 + sg_1z)^{-\frac{1}{s}-2}}{s^2 g_1^2} \left( s^2 g_1 z (g_2^2 - g_1 g_3) - sg_2^2 \ln(1 + sg_1z) + \frac{g_2^2}{2} (1 + s) \ln^2(1 + sg_1z) \right).$$

Here,  $g_j = -[\alpha^j] \gamma(\alpha)$  is the  $j^{\text{th}}$  coefficient of the anomalous dimension. These general results will subsequently be used to cross-check our calculation.

**2.5. MS scheme.** In the Minimal Subtraction scheme, the counter term  $\hat{Z}^{(m)}$  is chosen to contain only the pole terms in  $\epsilon$ , extracted by the operator  $\hat{\mathcal{R}}$ , of the integral at order  $m$ :

$$(2.21) \quad \hat{Z}^{(m)}(\epsilon) = \hat{Z}^{(m-1)}(\epsilon) - \hat{\mathcal{R}} \left[ \alpha \int dy K(x, y) Q \left( G^{(m-1)} \right) G^{(m-1)} \right] \quad (\text{MS scheme}).$$

In MS, the anomalous dimension  $\hat{\gamma}(\alpha)$  and the beta function  $\hat{\beta}(\alpha)$  are again defined as derivatives of the  $\hat{Z}$ -factors, eqs. (2.5) and (2.6). This implies, using eq. (2.7), that they do not depend on  $\epsilon$  at all:  $\hat{\beta}(\alpha, \epsilon) = \hat{\beta}(\alpha)$  and  $\hat{\gamma}(\alpha, \epsilon) = \hat{\gamma}(\alpha)$ . Further, the identity eq. (2.10),  $\hat{\beta}(\alpha) = s \hat{\gamma}(\alpha)$ , still holds if  $\hat{Q} = \hat{G}^s$ . The so-defined renormalization group functions fulfil once more the Callan-Symanzik equation 2.8 and its limit for  $\epsilon \rightarrow 0$ , eq. (2.13).

The MS-bar renormalization scheme is a variant of MS where those finite terms which arise from a series expansion of  $\frac{e^{\gamma_E}}{4\pi}$  are also subtracted. All quantities computed in Minimal Subtraction are denoted with hat like  $\hat{G}$ . We denote MS-bar quantities with a bar like  $\bar{G}$ . The undecorated quantities like  $G$  are in the MOM-scheme.

The MS-scheme involves a scale  $\mu$  in the definition of  $x = p^2/\mu^2$ , but no explicit condition of the Green function is imposed. The MS-renormalized Green function  $\hat{G}(\alpha, x)$  will be unity at some other scale  $p^2 = \hat{\mu}^2 = \delta(\alpha) \cdot \mu^2$ , where the factor  $\delta(\alpha)$  is itself a function of  $\alpha$ . One can view  $\delta(\alpha)$  as the renormalization point to be chosen in MOM in order to reproduce the MS Green function. A primary goal of the present work is to determine  $\delta(\alpha)$ .

### 3. MS AS A SHIFTED MOM SCHEME

**3.1. Shifted MOM renormalization point.** The formulas of section 2.4 are valid for MOM renormalization at  $x = 1$ . Now choose a kinematic renormalization point  $\delta^{-1} \neq 1$ . This is equivalent to choosing a reference momentum  $\mu' = \sqrt{\delta} \cdot \mu$  instead of  $\mu$  and using a new variable  $x' := p^2/\mu'^2 = \delta^{-1} \cdot x$  such that  $x = 1$  equals  $x' = \delta^{-1}$ . This setup is shown in fig. 1. The Green function  $G'(x')$  is defined by

$$(3.1) \quad G(\alpha, x) = G(\alpha, \delta \cdot x') =: G'(\alpha, x') = G'(\alpha, \delta^{-1} \cdot x).$$

It has a log-expansion (in the original variable  $x$ , not  $x'$ !) similar to eq. (2.15),

$$(3.2) \quad G'(x) = \gamma'_0(\alpha) + \sum_{k=1}^{\infty} \gamma'_k(\alpha) (\ln x)^k, \quad \gamma'_k = \sum_{j=k}^{\infty} \binom{j}{k} \gamma_j (\ln \delta)^{j-k}.$$

The first two of the new coefficients are, explicitly,

$$(3.3) \quad \gamma'_0(\alpha) = G'(\alpha, 1) = G(\alpha, \delta^{-1}), \quad \text{and} \quad \gamma'_1(\alpha) = x \partial_x G'(\alpha, x) \Big|_{x=1} = x \partial_x G(\alpha, x) \Big|_{x=\delta^{-1}}.$$

The new coefficients  $\gamma'_k(\alpha)$  do not fulfil the Callan-Symanzik equations 2.13 or 2.16, but instead

$$(3.4) \quad \begin{aligned} \gamma(\alpha) (1 + s\alpha\partial_\alpha) G'(\alpha, x') &= (1 + s\gamma(\alpha) \cdot \alpha\partial_\alpha \ln \delta(\alpha)) x' \partial_{x'} G'(\alpha, x') \\ \Rightarrow \gamma(\alpha) (1 + s\alpha\partial_\alpha) \gamma'_j(\alpha) &= (1 + s\alpha\gamma(\alpha)\partial_\alpha \ln \delta(\alpha))(j+1)\gamma'_{j+1}(\alpha). \end{aligned}$$

Importantly, the derivative  $\gamma'_1(\alpha)$  from eq. (3.3) is generally not the anomalous dimension  $\gamma'(\alpha)$  of the theory with shifted renormalization point, see fig. 1. Instead, the proper anomalous dimension respective beta function are, in the limit  $\epsilon \rightarrow 0$  from eq. (2.9),

$$(3.5) \quad \gamma'(\alpha) := \frac{\gamma(\alpha)}{1 + s\gamma(\alpha) \cdot \alpha\partial_\alpha \ln \delta(\alpha)}, \quad \beta'(\alpha) := s\gamma'(\alpha).$$

If the shift  $\delta$  of the renormalization point is independent from the renormalized coupling constant  $\alpha$ , then the derivative vanishes and indeed  $\gamma'_1(\alpha) = \gamma'(\alpha)$ . This situation amounts to a MOM scheme with a different, but fixed, renormalization point from the original scheme. If  $\delta(\alpha)$  does depend on  $\alpha$  (and  $s \neq 0$ ) then there are two effects: First,  $\gamma'_1(\alpha) \neq \gamma_1(\alpha)$  because these derivatives are taken at different points, see fig. 1, and second,  $\gamma'(\alpha) \neq \gamma(\alpha)$  because the moving renormalization point influences the Callan-Symanzik equation and the definition eq. (2.6). The latter is the situation we are facing when we interpret MS as a  $\alpha$ -dependent shifted MOM scheme below.

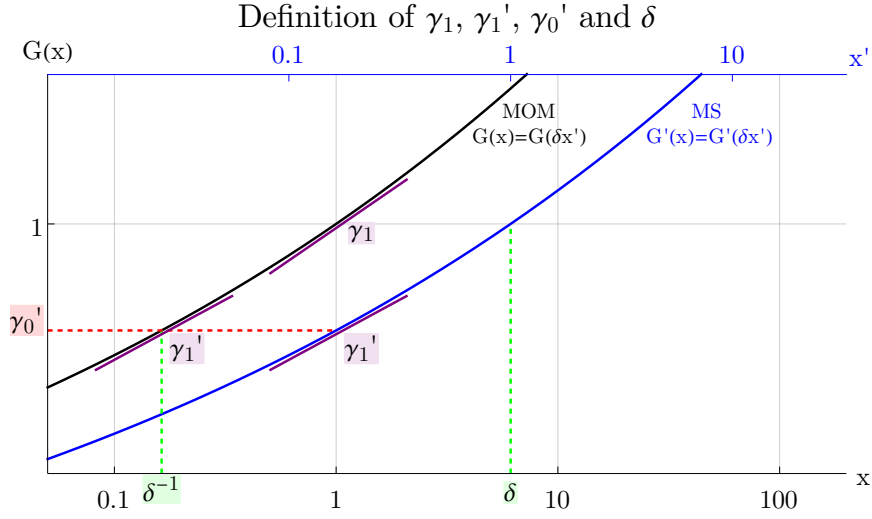


FIGURE 1. A hypothetical Green function in MOM ( $G(x)$ , black) and MS ( $G'(x)$ , blue). Both are initially given as functions of  $x$  (lower horizontal axis). We define a rescaled variable  $x' = x \cdot \delta^{-1}$  such that  $G'(x') = G(x)$ . This means that  $x = \delta$  (indicated in green) is the would-be kinematic renormalization point  $x' = 1$ . Conversely,  $\gamma'_0$  is the value  $G'(x = 1)$  (red). This equals  $G(x = \delta^{-1})$ . The derivative  $\gamma_1$  of  $G(x)$  at  $x = 1$  (purple) is different from the MS-derivative  $\gamma'_1$  at  $x = 1$ , which in turn equals the derivative of  $G(x)$  at  $x = \delta^{-1}$ . It is  $\gamma = \gamma_1$ , but the new anomalous dimension  $\gamma'$  does not have a graphical representation in this plot since it is not defined as a simple derivative of  $G'$  with respect to  $x$  or  $x'$ , see eq. (2.6).

**3.2. Linear case.** It is possible, in the limit  $\epsilon \rightarrow 0$ , to express the MS-renormalized Green function as a MOM-renormalized one where the renormalization point  $x = \delta^{-1}(\alpha)$  depends on the renormalized coupling  $\alpha$ . Note that the notion of “renormalization point” can either mean the value  $x = \delta^{-1}$  of  $x = p^2/\mu^2$  or equivalently the corresponding new scale  $\mu^2 \cdot \delta$ .

The goal of this paper is to determine  $\delta(\alpha)$ . If we were to know the exact MS-solution  $\hat{G}(\alpha, \hat{x})$  then this amounts to finding the point  $\hat{x} = \delta^{-1}(\alpha)$  where  $\hat{G}(\alpha, \delta^{-1}) = 1$ .

In the linear case,  $s = 0$ , the solution of the Callan-Symanzik equation eq. (2.13) is a monomial  $G(\alpha, x) = \gamma_0(\alpha)x^{\gamma(\alpha)}$ . In MOM, we have  $\gamma_0(\alpha) = 1$  by the renormalization condition eq. (2.12), and hence eq. (2.17). In MS, the solution will have some  $\hat{\gamma}_0(\alpha) \neq 1$ . Especially, the anomalous dimension  $\gamma(\alpha) = \hat{\gamma}(\alpha)$  is equal in both schemes by eq. (3.5) since  $s = 0$ . Using eq. (3.1), we find

$$(3.6) \quad (\delta(\alpha) \cdot x)^{\gamma(\alpha)} = \hat{\gamma}_0(\alpha)x^{\gamma(\alpha)} \quad \Rightarrow \quad \ln \delta(\alpha) = \frac{1}{\gamma(\alpha)} \ln \hat{\gamma}_0(\alpha).$$

The function  $\hat{\gamma}_0(\alpha)$  can be extracted from a known MS-solution  $\hat{G}(\alpha, x)$  via eq. (3.3).

It is also possible to infer  $\hat{\gamma}_0(\alpha)$  from the MOM-solution alone. To this end, note that the MS Green function is proportional to the one in MOM. Going back to the definition eq. (2.3) of the  $Z$ -factors, this means that  $\hat{Z}G_0 = \hat{\gamma}_0 \cdot ZG_0 + \mathcal{O}(\epsilon)$ . From the integral representation eq. (2.7), using that in MS  $\hat{\gamma}(\alpha, \epsilon) = \hat{\gamma}(\alpha)$ , we get

$$e^{-\int_0^\alpha \frac{du}{u} \frac{\hat{\gamma}(u)}{\epsilon}} = \hat{\gamma}_0(\alpha) \cdot e^{-\int_0^\alpha \frac{du}{u} \frac{\gamma(u, \epsilon)}{\epsilon}} + \mathcal{O}(\epsilon) \quad \Rightarrow \quad \gamma(\alpha, \epsilon) = \gamma(\alpha) + \epsilon \alpha \partial_\alpha \ln \hat{\gamma}_0(\alpha) + \mathcal{O}(\epsilon^2).$$

If we know the MOM anomalous dimension for  $\epsilon \neq 0$  then we can compute  $\hat{\gamma}_0$  and hence  $\ln \delta$  from

$$(3.7) \quad \alpha \partial_\alpha \ln \hat{\gamma}_0(\alpha) = [\epsilon^1] \gamma(\alpha, \epsilon).$$

In fact, for a linear DSE all coefficients of the MOM counter term  $Z(\alpha, \epsilon)$  are directly given by the  $\epsilon$ -expansion of the MOM anomalous dimension via eq. (2.7):

$$(3.8) \quad Z(\alpha, \epsilon) =: \exp \left( - \sum_{n=-1}^{\infty} \epsilon^n \cdot z_n(\alpha) \right), \quad \alpha \partial_\alpha z_n(\alpha) = [\epsilon^{n+1}] \gamma(\alpha, \epsilon), \quad z_0(\alpha) = \ln \hat{\gamma}_0(\alpha).$$

For the counter term  $\hat{Z}(\alpha, \epsilon)$  in MS, all  $\hat{z}_{n \geq 0}(\alpha)$  vanish, as do the  $\epsilon$ -dependent parts of  $\hat{\gamma}(\alpha, \epsilon) = \hat{\gamma}(\alpha)$ .

**3.3. Non-linear case.** We assume that we know the MOM- and the MS-solution and their corresponding counter terms, and hence the renormalization group functions, by explicit calculation. The remaining task is then to extract the shift  $\delta(\alpha)$  from this data. There are essentially three approaches.

The first approach utilizes the renormalization group equation eq. (3.4). If any two of the MS functions  $\hat{\gamma}_j(\alpha)$ , together with the MOM anomalous dimension  $\gamma(\alpha)$ , are known, then (for example using  $\hat{\gamma}_0$  and  $\hat{\gamma}_1$ )

$$(3.9) \quad \frac{\partial}{\partial \alpha} \ln \delta(\alpha) = \frac{\gamma \cdot \hat{\gamma}_0 - \hat{\gamma}_1}{s \alpha \cdot \hat{\gamma}_1} + \frac{1}{\hat{\gamma}_1} \frac{\partial}{\partial \alpha} \hat{\gamma}_0 \quad (\text{for } s \neq 0).$$

This allows to compute  $\delta(\alpha)$  up to the constant term.

The second approach is to compute all MS functions  $\hat{\gamma}_j(\alpha)$  up to some desired order  $j$  and additionally all MOM functions  $\gamma_j(\alpha)$ . Also, one writes a power series ansatz for  $\ln \delta(\alpha)$  and uses this to compute the powers  $(\ln \delta(\alpha))^k$ . Then the right side of eq. (3.2) is a linear system for the unknown coefficients of  $\ln \delta(\alpha)$  which can be solved up to the desired order.

The third approach utilizes the anomalous dimensions  $\gamma(\alpha)$  and  $\hat{\gamma}(\alpha)$ , which are known from the  $Z$ -factors  $Z_G(\alpha, \epsilon)$  and  $\hat{Z}_G(\alpha, \epsilon)$ . Inverting eq. (3.5) produces

$$(3.10) \quad \frac{\partial}{\partial \alpha} \ln \delta(\alpha) = \frac{1}{s\alpha} \left( \frac{1}{\hat{\gamma}(\alpha)} - \frac{1}{\gamma(\alpha)} \right).$$

**3.4. Fixing the constant term.** Some formulas leave open the constant term in  $\ln \delta(\alpha)$ . For the shift from MOM- to MS-renormalization, the constant term is fixed by the first order solution of the DSE. Let the primitive kernel Feynman integral of the DSE be  $\Gamma = (f^{-1}\frac{1}{\epsilon} + f_0 + f_1\epsilon + \dots)x^\epsilon$ . Then  $\alpha\Gamma$  is the first-order solution of the DSE and the anomalous dimension in MOM is  $\gamma(\alpha) = -\alpha f_{-1} + \mathcal{O}(\alpha^2)$ . On the other hand, in MS renormalization the value of  $G$  at  $x = 1$  is  $\hat{\gamma}_0 = 1 + \alpha f_0 + \mathcal{O}(\alpha^2)$ . Using eq. (3.2), this fixes the constant term of  $\ln \delta(\alpha)$ :

$$(3.11) \quad \ln \delta(\alpha) = -f_0(f_{-1})^{-1} + \mathcal{O}(\alpha).$$

Remarkably,  $\delta(0) = e^{-f_0/f_{-1}} \neq 1$  unless  $f_0 = 0$ , so the shift does not necessarily vanish for vanishing coupling. This result does not depend on the invariant charge in the DSE, or whether it is linear or non-linear, but just on the primitive kernel.

In the remainder of the paper, we will explicitly compute  $\delta(\alpha)$  for three different Dyson-Schwinger equations.

#### 4. LINEAR DSE IN $D = 4 - 2\epsilon$ DIMENSIONS

We first consider a linear Dyson-Schwinger equation of iterated one-loop Feynman graphs, namely

$$(4.1) \quad \hat{G}(q^2) = 1 + \lambda \int \frac{d^D k}{(2\pi)^D} \frac{\hat{G}(k^2)}{(k+q)^2 k^2} - \hat{\mathcal{R}} \left[ \lambda \int \frac{d^D k}{(2\pi)^D} \frac{\hat{G}(k^2)}{(k+q)^2 k^2} \right].$$

Here,  $\lambda$  is a coupling constant and  $D = 4 - 2\epsilon$  is the spacetime dimension. Equation (4.1) is the linear DSE (rainbow approximation) for the fermion propagator in Yukawa theory, but scaled and projected onto suitable tensors such that the order zero (tree level) solution is

$$(4.2) \quad \hat{G}^{(0)}(q^2) := 1.$$

**4.1. Computation of the coefficients.** One can solve the DSE eq. (4.1) to first order by inserting eq. (4.2) into it and computing the integrals according to appendix B:

$$(4.3) \quad \hat{G}^{(1)}(q^2) = 1 + \frac{\lambda}{(4\pi)^2} \left( 1 - \hat{\mathcal{R}} \right) \left[ (4\pi)^\epsilon e^{-\gamma_E \epsilon} \left( \frac{q^2}{m^2} \right)^{-\epsilon} \sum_{w=-1}^{\infty} f_w^{(0)} \epsilon^w \right].$$

Here,  $m^2$  is an arbitrary mass scale introduced for dimensional reasons and the coefficients  $f_w^{(k)}$  are given in eq. (B.2). The operator  $\hat{\mathcal{R}}$  projects the pole part of this equation, which is  $f_{-1}^{(0)} \epsilon^{-1}$ . This pole part is independent of momenta as expected in a locally renormalizable theory.

For a systematic treatment of higher orders, it will be advantageous to include the counter term as a summand  $\propto 1 = (q^2)^0$  into the solution. Define

$$\bar{g}_{1,w}^{(1)} := f_w^{(0)} \quad \bar{g}_{0,w}^{(1)} := \begin{cases} -f_{-1}^{(0)} & w = -1 \\ 0 & \text{else} \end{cases}$$

then the renormalized solution to order one, eq. (4.3), is

$$(4.4) \quad \hat{G}^{(1)}(q^2) = 1 + \frac{\lambda}{(4\pi)^2} \sum_{t=0}^1 (4\pi)^{t\epsilon} e^{-\gamma_E t\epsilon} \left( \frac{q^2}{m^2} \right)^{-t\epsilon} \sum_{w=-1}^{\infty} \bar{g}_{t,w}^{(1)} \epsilon^w.$$

The factor  $(4\pi)^{t\epsilon} e^{-\gamma_E t\epsilon}$  eventually produces finite contributions  $\propto \gamma_E$  and  $\propto \ln(4\pi)$ . In MS renormalization, these terms are present in the finite part of  $\hat{G}$  while in MS-bar renormalization they are assigned to the counter term  $\bar{Z}$  and thus absent from  $\bar{G}$ . To facilitate computations, we will absorb them into the momentum variable. This way, we effectively obtain the MS-bar Green function of the new momentum variable. On the other hand, our counter term will be  $\hat{Z}$  in MS as it does not contain the  $\ln(4\pi), \gamma_E$  contributions either. This way, we can skip in every intermediate step two additional series expansions, the ones of  $e^{-\gamma_E t\epsilon}$  and  $e^{\ln(4\pi)t\epsilon}$ . Let therefore

$$(4.5) \quad \hat{x} := \frac{q^2}{m^2}, \quad \bar{x} := \frac{e^{\gamma_E} q^2}{4\pi m^2} \equiv \frac{q^2}{\bar{m}^2}, \quad \hat{G}(\hat{x}) \equiv \bar{G}(\bar{x}).$$

The transition  $\hat{x} \leftrightarrow \bar{x}$  is a rescaling of the momentum which can also be understood as choosing a suitable value of the reference momentum  $m$ , as evidenced by the second equal sign where  $\bar{m}^2 = 4\pi e^{-\gamma_E} m^2$ . This is not kinematic renormalization:  $m$  merely tells how we measure momenta, the MS-renormalized Green function  $\hat{G}(q^2)$  does not fulfil any particular condition at the point  $q^2 = m^2$ . Also,  $m^2$  is not the mass of a particle, the field is still massless. Finally, let  $\alpha := \lambda(4\pi)^{-2}$ .

Higher orders of the renormalized Green function are computed iteratively. Assume that we know the solution to order  $(m-1)$ ,

$$\bar{G}^{(m-1)}(\alpha, \bar{x}) = \bar{G}^{(m-2)}(\alpha, \bar{x}) + \alpha^{m-1} \sum_{t=0}^{m-1} (\bar{x})^{-t\epsilon} \sum_{w=-(m-1)}^{\infty} \bar{g}_{t,w}^{(m-1)} \epsilon^w.$$

Inserting this into eq. (4.1), the order  $m$  solution is

$$(4.6) \quad \bar{G}^{(m)}(\alpha, \bar{x}) = \bar{G}^{(m-1)}(\alpha, \bar{x}) + \alpha^m \sum_{t=0}^m (\bar{x})^{-t\epsilon} \sum_{w=-m}^{\infty} \bar{g}_{t,w}^{(m)} \epsilon^w,$$

where the new coefficients are determined by

$$(4.7) \quad \bar{g}_{u,w}^{(m)} := \sum_{n=-m+1}^{w+1} \bar{g}_{u-1,n}^{(m-1)} f_{w-n}^{(u-1)} \quad \forall u > 0.$$

The counter term is included in this sum as the  $t=0$  summand. The coefficient of order  $\epsilon^w$  in the MS-counter term at  $m$  loops is

$$(4.8) \quad \bar{g}_{0,w}^{(m)} = - \sum_{u=1}^m \bar{g}_{u,w}^{(m)} \quad \text{if } w \in \{-m, \dots, -1\}, \text{ and } \bar{g}_{0,w}^{(m)} = 0 \text{ for all other } w.$$

The all-order perturbative solution  $\bar{G}(\bar{x})$  of eq. (4.1) is defined as the limit  $m \rightarrow \infty$  in eq. (4.6), effectively it is an infinite sum over the orders  $\alpha^m$  in the coupling. We exchange the sums to expose the expansion eq. (2.15) and the counter term  $\hat{Z}$ :

$$(4.9) \quad \bar{G}(\alpha, \bar{x}) = \hat{Z}(\alpha, \epsilon) + \sum_{k=0}^{\infty} \ln(\bar{x})^k \sum_{t=1}^{\infty} \frac{(-t)^k}{k!} \sum_{m=t}^{\infty} \alpha^m \sum_{w=-m}^{\infty} \bar{g}_{t,w}^{(m)} \epsilon^{k+w}.$$

As explained above eq. (4.5), we have introduced the MS (not MS-bar) counter term,

$$(4.10) \quad \hat{Z}(\alpha, \epsilon) := 1 + \sum_{m=1}^{\infty} \alpha^m \sum_{w=-m}^{-1} \bar{g}_{0,w}^{(m)} \epsilon^w = 1 - \sum_{m=1}^{\infty} \alpha^m \sum_{w=-m}^{-1} \sum_{t=1}^m \bar{g}_{t,w}^{(m)} \epsilon^w.$$

The eqs. (4.9) and (4.10) together with the recursion relations eqs. (4.7) and (4.8) allow us to compute the solution of the DSE 4.1 to arbitrary order.

A similar procedure can be used to obtain the MOM-renormalized finite Green function  $G(\bar{x})$ . One merely has to extend eq. (4.7) to include all orders  $w$  of  $\epsilon$ . If we are only interested in the

finite (as  $\epsilon \rightarrow 0$ ) part, then, in a linear DSE, it is sufficient to include the  $w = 0$  term into the counter term. To this end, instead of eqs. (4.7) and (4.8) one uses

$$(4.11) \quad g_{u,w}^{(m)} := \begin{cases} \sum_{n=-m+1}^{w+1} g_{u-1,n}^{(m-1)} f_{w-n}^{(u-1)} & \forall u > 0 \\ -\sum_{u=1}^m g_{u,w}^{(m)} & \text{if } u = 0 \text{ and } w \in \{-m, \dots, 0\}, \text{ and } 0 \text{ else.} \end{cases}$$

The counter term computed by eq. (4.11) is not the ‘‘true’’ counter term of kinematic renormalization. But this prescription produces a MOM-renormalized finite Green function

$$(4.12) \quad G(\alpha, \bar{x}) = Z(\alpha, \epsilon) + \sum_{k=0}^{\infty} \ln(\bar{x})^k \frac{1}{k!} \sum_{m=t}^{\infty} \alpha^m \sum_{t=1}^{\infty} (-t)^k \sum_{w=-m}^{\infty} g_{t,w}^{(m)} \epsilon^{k+w}$$

which by construction takes the value unity at the renormalization point  $\bar{x} = 1$ , i.e. at the momentum  $q^2 = \mu^2$ . Now the interpretation of  $\mu^2$  has changed: In the MS- or MS-bar-solutions, it was an arbitrary momentum scale without any particular meaning for the Green function while in MOM it is the momentum where  $G(\alpha, q^2/\mu^2) = 1$ .

**4.2. Renormalized correlation function.** In MOM renormalization, the analytic solution of the this linear DSE has long been known [23]. As always for a linear DSE, it is a pure scaling solution where the anomalous dimension  $\gamma(\alpha)$  is determined from the Mellin transform of the primitive, see eq. (2.18) and appendix A. With the notation of eq. (2.15), the MOM-solution at  $\epsilon = 0$  reads

$$(4.13) \quad G(\alpha, \bar{x}) = \bar{x}^{\gamma(\alpha)}$$

where  $\gamma_0(\alpha) = 1$ ,  $\gamma(\alpha) = \frac{\sqrt{1-4\alpha}-1}{2} = -\sum_{n=1}^{\infty} C_{n-1} \alpha^n$ ,  $\gamma_k(\alpha) = \frac{1}{k!} (\gamma(\alpha))^k$ .

Here,  $C_n$  are the Catalan numbers. It has been verified symbolically up to order  $\alpha^{25}$  that the series eq. (4.12) indeed coincides with eq. (4.13) in the limit  $\epsilon \rightarrow 0$ .

In MS-bar-renormalization, there is a finite remainder term in the  $\epsilon^0$ -coefficient of each order in  $\alpha$ , which would have been subtracted in kinematic renormalization. Therefore, the MS-bar-coefficients  $\bar{\gamma}_k(\alpha)$  in eq. (2.15) are generally different from the MOM-coefficients  $\gamma_k(\alpha)$ , see section 3.1. We compute  $\delta(\alpha)$  from  $\bar{\gamma}_0(\alpha)$  via eq. (3.6). From eq. (4.9) one reads off

$$(4.14) \quad \bar{\gamma}_0(\alpha) = 1 + \sum_{m=1}^{\infty} \alpha^m \sum_{t=1}^m \bar{g}_{t,0}^{(m)} = 1 + 2\alpha + \frac{11}{2}\alpha^2 + \frac{51-2\zeta(3)}{3}\alpha^3 + \frac{1341-80\zeta(3)}{24}\alpha^4 + \mathcal{O}(\alpha^5).$$

We have used that the  $\hat{Z}$ -factor in MS has, at finite order, only terms singular in  $\epsilon$  and therefore does not contribute to  $\bar{\gamma}_k$  and the summand  $t = 0$  can be left out. For the interpretation as a change of renormalization point, the remaining functions  $\bar{\gamma}_k(\alpha)$  have to be consistent with eqs. (3.2) and (4.13). It has been verified to order  $\alpha^{25}$  and for  $k \leq 15$  that indeed  $\bar{\gamma}_k(\alpha) = \bar{\gamma}_0(\alpha) \cdot \gamma_k(\alpha)$ .

Remarkably, for the linear DSE eq. (4.1) considered here, it is possible to find a closed formula for  $\bar{\gamma}_0(\alpha)$ . To do this, one computes the logarithm of the series eq. (4.14) and repeatedly uses the OEIS [38]. One can first identify the rational coefficients and their generating function. Subtracting that part one is left with

$$\begin{aligned} \ln \bar{\gamma}_0 - \ln \left( \frac{1 - \sqrt{1-4\alpha}}{2\alpha(1-4\alpha)^{\frac{1}{4}}} \right) &= -\zeta(3) \left( 2\frac{\alpha^3}{3} + 8\frac{\alpha^4}{4} + 30\frac{\alpha^5}{5} + 112\frac{\alpha^6}{6} + 420\frac{\alpha^7}{7} + 1584\frac{\alpha^8}{8} + \dots \right) \\ &\quad - \zeta(5) \left( 2\frac{\alpha^5}{5} + 12\frac{\alpha^6}{6} + 56\frac{\alpha^7}{7} + 240\frac{\alpha^8}{8} + 990\frac{\alpha^9}{9} + \dots \right) - \zeta(7) \dots \end{aligned}$$

At least up to  $\zeta(11)$  and  $\alpha^{25}$ , the coefficients of  $\frac{\alpha^{j+m-1}}{j+m-1}$  in the term proportional to  $\zeta(m)$  are given by the binomial coefficient  $2^{\binom{2j+m-3}{j-1}}$ . Assuming again that this holds universally, all series over  $\alpha$  and then the remaining series in  $\zeta(m)$  can be summed and yield known functions. The result is

$$(4.15) \quad \bar{\gamma}_0(\alpha) = e^{\gamma_E(1-\sqrt{1-4\alpha})} \frac{1 - \sqrt{1-4\alpha} \Gamma\left(\frac{3}{2} - \frac{1}{2}\sqrt{1-4\alpha}\right)}{2\alpha(1-4\alpha)^{\frac{1}{4}} \Gamma\left(\frac{1}{2} + \frac{1}{2}\sqrt{1-4\alpha}\right)} = \frac{-\gamma}{\alpha} \sqrt{\frac{d(-\gamma)}{d\alpha}} e^{-2\gamma\gamma_E} \frac{\Gamma(1-\gamma)}{\Gamma(1+\gamma)}.$$

In the latter form,  $\gamma \equiv \gamma(\alpha)$  is the anomalous dimension from eq. (4.13).

With this function  $\bar{\gamma}_0(\alpha)$  and eq. (4.13), the MS-bar-renormalized solution  $\bar{G}(\bar{x})$  in the limit  $\epsilon \rightarrow 0$  reads explicitly

$$(4.16) \quad \bar{G}(\alpha, \bar{x}) = \bar{\gamma}_0(\alpha) \cdot G(\alpha, \bar{x}) = \bar{\gamma}_0(\alpha) \cdot \bar{x}^{\gamma(\alpha)}.$$

From eq. (4.5) one can reconstruct the MS-renormalized function  $\hat{G}(\hat{p}^2)$ :

$$(4.17) \quad \hat{G}(\alpha, \hat{x}) = \bar{G}\left(\alpha, \frac{\hat{x}}{4\pi e^{-\gamma_E}}\right) = \hat{\gamma}_0(\alpha) \cdot \hat{x}^{\gamma(\alpha)} \quad \text{where} \quad \hat{\gamma}_0(\alpha) := (4\pi e^{-\gamma_E})^{-\gamma(\alpha)} \cdot \bar{\gamma}_0(\alpha)$$

Following section 3.1, the correspondence between MS-, MS-bar- and MOM-renormalized Green functions can equivalently be expressed by their respective renormalization points. Let  $\mu$  be the mass scale in MS- and MS-bar-renormalization. Then the Green function is unity at  $x = \hat{\delta}^{-1}$  and  $x = \bar{\delta}^{-1}$ , respectively. Equivalently,  $\hat{\mu}^2 = \hat{\delta} \cdot \mu^2$  and  $\bar{\mu}^2 = \bar{\delta} \cdot \mu^2$  are the mass scales one needs to choose for MS and MS-bar, in order to reproduce kinematic renormalization at the scale  $\mu^2$ :

$$G\left(\alpha, \frac{q^2}{\mu^2}\right) \equiv \bar{G}\left(\alpha, \frac{q^2}{\bar{\mu}^2}\right) \equiv \hat{G}\left(\alpha, \frac{q^2}{\hat{\mu}^2}\right).$$

By eqs. (3.6), (4.13) and (4.15), these scales are related via

$$(4.18) \quad \bar{\delta}(\alpha) = \bar{\gamma}_0^{\frac{1}{\gamma}} = e^{-2} \left(1 - \frac{3}{2}\alpha - \left(\frac{49}{24} - \frac{2}{3}\zeta(3)\right)\alpha^2 + \mathcal{O}(\alpha^3)\right), \quad \hat{\delta}(\alpha) = \hat{\gamma}_0^{\frac{1}{\gamma}} = \frac{\bar{\delta}(\alpha)}{\sqrt{4\pi e^{-\gamma_E}}}.$$

The latter of course reproduces the transformation  $m \leftrightarrow \bar{m}$  in eq. (4.5). The zeroth order coefficient is  $e^{-2}$  as expected from eq. (3.11) where  $f_{-1} = f_{-1}^{(0)} = 1$ ,  $f_0 = f_0^{(0)} = 2$ . In any case, the shift between renormalization schemes is a finite function as long as  $\alpha < \frac{1}{4}$ , shown in fig. 2.

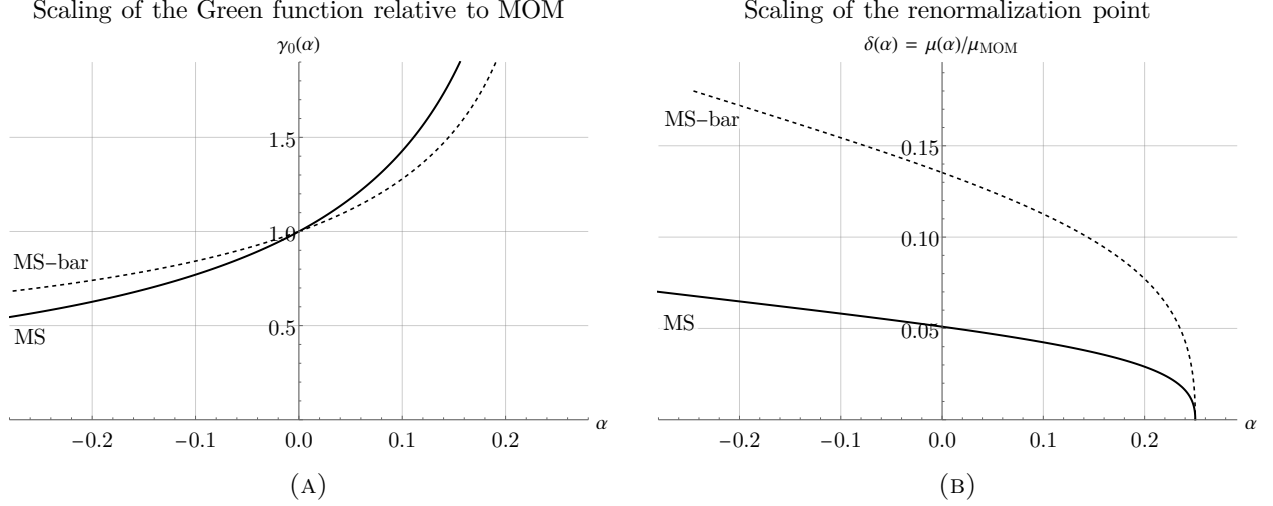


FIGURE 2. (A) Behaviour of the MS scaling-function  $\hat{\gamma}_0(\alpha)$  (thick) and the MS-bar scaling function  $\bar{\gamma}_0(\alpha)$  (dashed) as functions of the renormalized coupling  $\alpha$ . Both are unity at  $\alpha = 0$  and diverge at  $\alpha = \frac{1}{4}$ . (B) Rescaling factor  $\delta(\alpha)$  according to section 3.1 of the reference momentum in MS-renormalization  $\hat{\mu}$  (thick) and MS-bar-renormalization  $\bar{\mu}$  (dashed) relative to the MOM-renormalization-point  $\mu$ . The functions are equal up to the factor  $\sqrt{4\pi e^{-\gamma_E}}$ . They are not unity for  $\alpha = 0$ .

**4.3. Counter term and  $\epsilon$ -dependence.** Our calculation (up to order  $\alpha^{25}$ ) delivers for the counter term in MS the series coefficients

$$\ln \left( \hat{Z}(\alpha, \epsilon) \right) = -\frac{1}{\epsilon} \left( \alpha + \frac{\alpha^2}{2} + 2\frac{\alpha^3}{3} + 5\frac{\alpha^4}{4} + 14\frac{\alpha^5}{5} + 42\frac{\alpha^6}{6} + \dots \right).$$

Once more we recognize the Catalan numbers and introduce  $\gamma = \gamma(\alpha)$  from eq. (4.13),

$$(4.19) \quad \hat{Z}(\alpha, \epsilon) = \exp \left( -\frac{1}{\epsilon} \sum_{m=1}^{\infty} C_{m-1} \frac{\alpha^m}{m} \right) = e^{-\frac{1}{\epsilon} \left( 1 - \sqrt{1-4\alpha} + \ln \left( 1 - \frac{1-\sqrt{1-4\alpha}}{2} \right) \right)} = e^{\frac{1}{\epsilon} (2\gamma - \ln(1+\gamma))}.$$

This expression is the integral of  $\gamma(\alpha)$ , as expected from eq. (2.7) for a linear DSE. As long as  $\alpha$  and  $\epsilon$  have the same sign, this function has the limit  $\hat{Z}(\alpha, 0^+) = 0$  when  $\epsilon \rightarrow 0$ , see fig. 3. With eq. (4.19), the counter term turns out to be a remarkably well-behaved function of  $\epsilon$ , compared to its perturbative expansion, where every single term diverges as  $\epsilon \rightarrow 0$ . This is in line with [33] and a comment made in [29]: The all-order-solution eq. (4.13) “regulates itself” by its anomalous dimension. The integral in the DSE eq. (4.1) is not divergent and the remaining finite counter term is set to zero in MOM by choice of the renormalization point. Figure 3 shows how  $\hat{Z}$  approaches zero as the scaling solution  $\epsilon = 0$  is reached.

Using the expansion eq. (3.8), it has been verified to order  $\alpha^{20}$  that  $z_{-1}(\alpha) = \bar{z}_{-1}(\alpha)$  is given by  $\gamma(\alpha) = \bar{\gamma}(\alpha)$  and that the MOM-coefficient  $z_0(\alpha)$  fulfils  $z_0(\alpha) = \ln \bar{\gamma}_0(\alpha)$  as expected. In our pseudo-MOM-scheme eq. (4.11), all other  $z_{n>0}$  vanish. In true kinematic renormalization, they are present. The author computed the coefficients  $z_{n \leq 9}$  up to order  $\alpha^{10}$  but did not succeed in finding generating functions. However it turned out that all  $z_{n \leq 9}(\alpha)$  for  $0 < \alpha < \frac{1}{4}$  are, within the computed order, strictly positive. This implies that the exponent is strictly negative for all  $\epsilon > 0$  and hence  $Z(\alpha, \epsilon) \in [0, 1]$ . The classical interpretation of the  $Z$ -factor as a probability requires these bounds. Compare [27, Sec 8] for the various interpretations of  $Z$  and their relations.

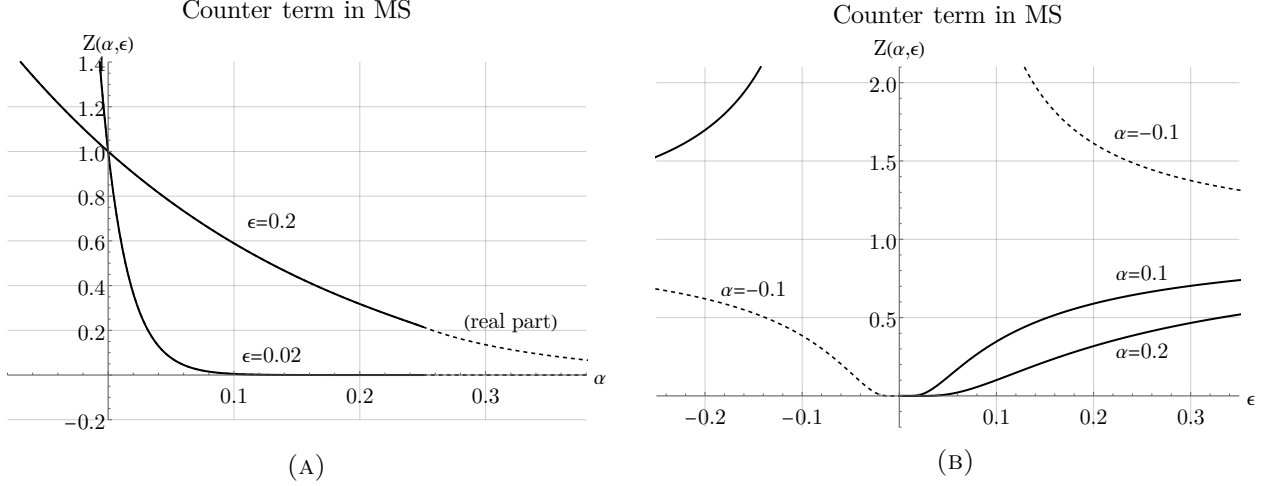


FIGURE 3. (A) Counter term  $\hat{Z}(\alpha, \epsilon)$  in MS as a function of the renormalized coupling  $\alpha$  for different values of  $\epsilon$ . As  $\epsilon \rightarrow 0^+$ , the function approaches zero for  $\alpha > 0$  and diverges for  $\alpha < 0$ . For  $\alpha > \frac{1}{4}$ , the counter term acquires an imaginary part which is not shown. (B) The same counter term as a function of  $\epsilon$  for fixed values of  $\alpha$ . For positive  $\alpha$ , the counter term smoothly approaches the value zero as  $\epsilon \rightarrow 0^+$ .

## 5. LINEAR DSE IN $D = 6 - 2\epsilon$ DIMENSIONS

For the 6-dimensional case, the procedure is completely analogous to the one described in the previous section. We will use the same symbols as in the  $D = 4$  case in order to not clutter notation.

The Dyson-Schwinger equation is once more eq. (4.1), only now with  $D = 6 - 2\epsilon$ . This time, we define  $\alpha := \lambda(4\pi)^{-3}$  to account for the additional factor  $4\pi$  produced by the integration. Moreover, the 1-loop-integral is now proportional to  $q^2$  but this factor is absorbed by projection onto the basis tensor such that again the tree level solution is  $G^{(0)}(q^2) = 1$ . Then, the coefficients of the renormalized Green function and the counter term are given by the same recursion relations as above, namely eqs. (4.7), (4.8) and (4.11). The crucial difference is that for  $f_n^{(k)}$  one now takes the value of the 6-dimensional primitive integral, as given in eq. (B.3).

Once more, the anomalous dimension can be computed analytically from the Mellin transform of the 1-loop integral appendix A. The Green function in kinematic renormalization is [22]

$$G(\bar{x}) = \bar{x}^{\gamma(\alpha)}, \quad \gamma(\alpha) = \frac{\sqrt{5 + 4\sqrt{1 + \alpha}} - 3}{2}.$$

The functions  $\bar{\gamma}_k(\alpha)$  are again computed from eq. (4.9) using the appropriate  $\bar{g}_{t,s}^{(m)}$ . Like above, all  $\bar{\gamma}_k(\alpha)$  are proportional to the corresponding  $\gamma_k(\alpha)$  at least up to  $\alpha^{25}$  and  $k = 20$ .

The series coefficients of  $\bar{\gamma}_0(\alpha)$  can no longer be identified from tables right away but the result eq. (4.15), expressed in terms of  $\gamma(\alpha)$ , is a helpful starting point. Eventually, one arrives at

$$(5.1) \quad \bar{\gamma}_0(\alpha) = 3\sqrt{3} \frac{e^{\frac{1}{2}(\sqrt{5+4\sqrt{1+\alpha}}-3)(1-2\gamma_E)} (\sqrt{5+4\sqrt{1+\alpha}}-3) \Gamma\left(\frac{5}{2} - \frac{1}{2}\sqrt{5+4\sqrt{1+\alpha}}\right)}{\alpha ((1+\alpha)(5+4\sqrt{1+\alpha}))^{\frac{1}{4}} \Gamma\left(-\frac{1}{2} + \frac{1}{2}\sqrt{5+4\sqrt{1+\alpha}}\right)}$$

$$= \frac{6\gamma}{\alpha} \sqrt{\frac{d(6\gamma)}{d\alpha}} e^{\gamma(1-2\gamma_E)} \frac{\Gamma(1-\gamma)}{\Gamma(1+\gamma)}.$$

This has been verified symbolically to order  $\alpha^{25}$ . Knowing  $\bar{\gamma}_0(\alpha)$ , the shifts between MS-bar- resp. MS- and MOM-renormalization are  $\bar{\delta}(\alpha) = \bar{\gamma}_0^{\frac{1}{\gamma}}$  and  $\hat{\delta}(\alpha) = (4\pi e^{-\gamma})^{-\frac{1}{2}} \bar{\delta}(\alpha)$ .

The counter term in MS for the 6-dimensional theory is

$$\hat{Z}(\alpha, \epsilon) = e^{\frac{1}{\epsilon} \left( 2\sqrt{5+4\sqrt{1+\alpha}} - 6 - \frac{3}{2} \ln \alpha + \ln(108) + \frac{1}{2} \ln \frac{\sqrt{5+4\sqrt{1+\alpha}}-1}{\sqrt{5+4\sqrt{1+\alpha}+1}} + \frac{3}{2} \ln \frac{\sqrt{5+4\sqrt{1+\alpha}}-3}{\sqrt{5+4\sqrt{1+\alpha}+3}} \right)}.$$

This function fulfills eq. (2.7). Furthermore, it has been checked to order  $\alpha^{25}$  resp.  $\alpha^{10}$  that  $Z(\alpha, \epsilon)$  reproduces  $\bar{\gamma}_0$  via eq. (3.8) for the pseudo-MOM and the true MOM scheme, respectively.

## 6. KREIMER'S LINEAR TOY MODEL

Both Dyson-Schwinger equations considered above were based on the same 1-loop primitive Feynman graph as an integral kernel. Our formalism is not restricted to that particular integral, for comparison we here examine the linear Dyson-Schwinger equation in a toy model of renormalization proposed by Dirk Kreimer [35]. It reads

$$(6.1) \quad \hat{G}(\alpha, x) = 1 + \left(1 - \hat{\mathcal{R}}\right) \alpha \int_0^\infty \frac{dy (xy)^{-\epsilon}}{1+y} \hat{G}(\alpha, xy),$$

where again  $\epsilon$  is a regularization parameter. There is no distinction between MS- and MS-bar schemes in the toy model. We retreat to a comparison between MS and pseudo-MOM.

The anomalous dimension, computed from the Mellin transform eq. (2.18) and appendix A, is

$$\gamma(\alpha) = -\frac{1}{\pi} \arcsin(\pi\alpha) = -\alpha - \frac{\pi^2}{6} \alpha^3 - \frac{3\pi^4}{40} \alpha^5 - \frac{5\pi^6}{112} \alpha^7 - \dots$$

It has been verified to order  $\alpha^{30}$  that the symbolic calculation of  $G(\alpha, x)$  in pseudo-MOM renormalization produces, in the limit  $\epsilon \rightarrow 0$ , the expansion coefficients of  $x^{\gamma(\alpha)}$  from eq. (2.17).

For MS, using [38, A034255], the scaling factor is

$$(6.2) \quad \hat{\gamma}_0(\alpha) = 1 + \sum_{m=1}^{\infty} \alpha^m \sum_{t=1}^m \hat{g}_{t,0}^{(m)} = 1 + \left(\frac{\pi^2 \alpha^2}{4}\right) + \frac{5}{2} \left(\frac{\pi^2 \alpha^2}{4}\right)^2 + \dots = (1 - \pi^2 \alpha^2)^{-\frac{1}{4}} = \sqrt{\frac{d\gamma}{d\alpha}}.$$

From this, the change of the renormalization point can be computed using eq. (3.6). One finds

$$\ln \hat{\delta}(\alpha) = \frac{\pi \ln(1 - \alpha^2 \pi^2)}{4 \arcsin(\alpha\pi)} = -\frac{\pi^2}{4} \alpha - \frac{\pi^4}{12} \alpha^3 - \frac{73\pi^6}{1440} \alpha^5 - \mathcal{O}(\alpha^7),$$

where the constant coefficient vanishes since for the toy model  $f_0 = f_0^{(0)} = 0$ .

The series coefficients of the toy model are somewhat easier than for the physical theory. This entails that in the expansion

$$(6.3) \quad Z(\alpha, \epsilon) \equiv \exp\left(-\sum_{n=1}^{\infty} z_n(\alpha) \cdot \epsilon^n\right) \equiv \exp\left(\sum_{n=1}^{\infty} z'_n(\epsilon) \cdot \alpha^n\right).$$

the functions  $z_n(\alpha)$  and  $z'_n(\alpha)$  can be found symbolically. Some of them are quoted in appendix C for the interested reader. They suggest that  $Z(\alpha, \epsilon) \in [0, 1]$ . As expected from eq. (3.8), also the linear toy model fulfils

$$z_{-1} = -[\epsilon^{-1}] \ln Z = -\int_0^\alpha \frac{du}{u} \gamma(u), \quad z_0 = -[\epsilon^0] \ln Z = -\frac{1}{4} \ln(1 - \alpha^2 \pi^2) = \ln \bar{\gamma}_0(\alpha).$$

## 7. NON-LINEAR DSE IN $D = 4$

In the remainder of the paper we repeat the above analysis of the two physical models and the toy model for the case that the Dyson-Schwinger equation is non-linear. Namely, instead of  $Q \equiv 1$  we insert the invariant charge eq. (2.2),

$$(7.1) \quad Q(G(\alpha, x)) = (G(\alpha, x))^s,$$

where  $s \in \{-5, \dots, +5\}$ . It seems that the literature so far has mostly concentrated on the physically most relevant cases  $s = 0$  (linear approximation, e.g. [23, 22, 29]) and  $s = -2$  (one inverse Green function inserted into the kernel, e.g. [12, 13, 6, 5, 7, 11, 9]). In our case, the corresponding power of  $G$  is inserted into *only one* edge of the primitive. The setup discussed in [6, 5, 7] is conceptually different from our  $s = -3$  since it amounts to inserting one  $G^{-2}$  into each of the two internal edges. Compare our result eq. (7.6) with [6, Table 1]. Also see [40, Sec. 5] for a discussion how insertion into only a subset of the available edges is equivalent to including additional primitive kernels.

**7.1. Computation of the coefficients.** The MS-renormalized Dyson-Schwinger equation for the  $D = 4$  model reads

$$(7.2) \quad \hat{G}(\alpha, q^2/\mu^2) = 1 + \alpha(4\pi)^2 \left(1 - \hat{\mathcal{R}}\right) \int \frac{d^D k}{(2\pi)^D} \frac{\left(\hat{G}(\alpha, k^2/\mu^2)\right)^{s+1}}{(k+q)^2 k^2}.$$

Note that as above we choose a sign  $+\alpha$  in front of the integral. For  $s = -2$ , this is the model examined in [12, 13, 11], up to a factor -2 in the definition of  $\alpha$ , see [13, eq. (12)].

For a recursive computation of the coefficients, we once more introduce  $\hat{x}, \bar{x}$  according to eq. (4.5) and thereby switch from MS- to MS-bar-renormalization. The first order solution coincides with the one of the linear DSE, eq. (4.4),

$$\bar{G}^{(1)}(\alpha, \bar{x}) = 1 + \alpha \sum_{t=0}^1 \bar{x}^{-t\epsilon} \sum_{w=-1}^{\infty} \bar{g}_{t,w}^{(1)} \epsilon^w.$$

The index  $^{(m)}$  in the linear case counts both the coradical degree (= number of recursive iteration of the solution) and the order in  $\alpha$  (= loop number of the involved graphs). In the non-linear DSE, we truncate the series expansion of  $\left(\hat{G}(\alpha, \bar{x})\right)^{s+1}$  at order  $\alpha^{m-1}$  so that  $\hat{G}^{(m)}(\alpha, \bar{x})$  again involves Graphs with at most  $m$  loops. This choice is arbitrary but convenient because it saves one index.

The recursion formula for the next order is more complicated than in the linear case section 4.1. This is because the non-linear DSE eq. (7.2) involves a non-trivial power of the Green function inside the integral which needs to be expanded both in  $\alpha$  and in  $\bar{x}^{-\epsilon}$ . Assume we know the order- $m$ -solution in the form

$$\bar{G}^{(m)}(\alpha, \bar{x}) = 1 + \sum_{n=1}^m \alpha^n \sum_{u=0}^n \bar{x}^{-u\epsilon} \sum_{s=-n}^{\infty} \bar{g}_{u,w}^{(n)} \epsilon^w =: 1 + \sum_{n=1}^m \alpha^n \bar{G}_n(\bar{x}, \epsilon),$$

where we defined functions  $\bar{G}_n(\bar{x}, \epsilon)$ . They are universal for all  $m$ . Next, we write a generic expansion of the invariant charge eq. (7.1) according to

$$(7.3) \quad \bar{G}^{(m)}(\alpha, \bar{x}) \cdot Q(\bar{G}^{(m)}(\alpha, \bar{x})) \equiv \left(\bar{G}^{(m)}(\alpha, \bar{x})\right)^{s+1} =: 1 + \sum_{n=1}^m \alpha^n \sum_{t=0}^n \bar{x}^{-t\epsilon} \bar{h}_t^{(n)}(\epsilon).$$

The helper functions  $\bar{h}_t^{(n)}(\epsilon)$  are Laurent series in  $\epsilon$  with the highest pole order  $\epsilon^{-n}$ . They are given by Faa di Bruno's formula and the Binomial theorem,  $B_{n,k}$  are Bell polynomials[4] [18, p 134]:

$$(7.4) \quad \begin{aligned} \frac{1}{(\bar{G}^{(m)}(\bar{x}))^{-s-1}} &= \frac{1}{(-s-2)!} \sum_{n=0}^{\infty} \alpha^n \frac{1}{n!} \sum_{k=1}^n (-s-2+k)! B_{n,k} (1!\bar{G}_1, 2!\bar{G}_2, \dots), \quad s < -1 \\ (\bar{G}^{(m)}(\bar{x}))^{s+1} &= (s+1)! \sum_{n=0}^{\infty} \alpha^n \frac{1}{n!} \sum_{k=0}^{s+1} \frac{1}{(s+1-k)!} B_{n,k} (1!\bar{G}_1, 2!\bar{G}_2, \dots), \quad s > -1. \end{aligned}$$

Knowing the functions  $\bar{h}_t^{(n)}(\epsilon)$ , one integrates the sum eq. (7.3) term-wise like in the linear case section 4.1 and obtains the next-order coefficients

$$\bar{g}_{1,w}^{(1)} = f_w^{(0)}, \quad \bar{g}_{u,w}^{(n)} = \sum_{r=-1}^{n+w-1} \left( [\epsilon^{w-r}] \bar{h}_{u-1}^{(n-1)} \right) f_r^{(u-1)}.$$

Finally, one obtains the next order solution of the DSE,

$$(7.5) \quad \bar{G}^{(m+1)}(\alpha, \bar{x}) = \bar{G}^{(1)}(\alpha, \bar{x}) + (1 - \hat{\mathcal{R}}) \sum_{n=2}^{m+1} \alpha^n \sum_{u=1}^n \bar{x}^{-u\epsilon} \sum_{w=-n}^{\infty} \bar{g}_{u,w}^{(n)} \epsilon^w.$$

The MS-counter term is included via coefficients  $g_{0,s}^{(n)}$  as in the linear case eq. (4.8). For the non-linear DSE, there is no simple pseudo-MOM scheme. In practice, it is sufficient to include terms  $\propto \epsilon^m$  if one is interested in the finite part of the Green function  $G^{(m)}(\alpha, \bar{x})$  since every iteration potentially multiplies the result with  $\epsilon^{-1}$ .

Of course, the established methods [12, 30, 5] are tremendously more efficient in computing the anomalous dimension in MOM. A power-series solution of the ODE eq. (7.7) to order  $\alpha^{100}$  can be obtained within seconds while the brute-force algorithm merely reaches  $\alpha^{10}$  symbolically after several hours. But the computation of  $\gamma(\alpha)$  is only a side effect of our algorithm since we are actually interested in  $\ln \delta(\alpha)$ .

All computations, also the extraction of series coefficients in the computation of  $h_t^{(n)}$  and  $g_{u,w}^{(n)}$ , have been done with the computer algebra system Mathematica 12.3. In practice, the computation is entirely limited by CPU time due to an explosion of series coefficients: In order to reach  $\epsilon^0$  at order  $\alpha^{10}$ , we have to include terms up to  $\epsilon^{10}$  in the intermediate steps. Further we produce pole terms up to  $\epsilon^{-10}$  and contributions up to  $x^{-10\epsilon}$ , each  $g_{t,s}^{(10)}$  requires series reversion and -multiplication. If we were to go to  $\alpha^{20}$ , we would have to include  $\epsilon^{20}$  from the start, dramatically slowing down every intermediate step.

The higher the order, the higher powers of  $\pi^2$  and the more different zeta values appear. Algebraic operations with these expressions are increasingly slow. This second problem can be circumvented by working with floating point numbers, but it turns out that each iteration loses several decimal digits of precision. We computed the first orders symbolically and then continued numerically.

Thirdly, the expansions eq. (7.4) are, for large  $n$ , much harder for negative  $s$  than for small positive  $s$  due to the summation boundaries. Therefore we reach higher order for the positive  $s$ .

**7.2. Results.** The coefficients were computed symbolically up to  $\alpha^{10}$  for an invariant charge eq. (7.1) where  $s \in \{-5, \dots, +5\}$ . The results are extended up to at least  $\alpha^{20}$  numerically with at least 30 valid decimal digits. It was verified in all cases that the first three orders of the leading-log expansion fulfil eq. (2.20) and that eq. (3.4) holds.

The anomalous dimensions up to order  $\alpha^8$  are reported in table 6 in appendix E. Let the anomalous dimension be  $\gamma(\alpha) = \sum_{n=0}^{\infty} c_n \alpha^n$  then the empirical values of table 6 suggest  $c_0 = 0, c_1 =$

$-1, c_2 = -(s+1), c_3 = -(1+s)(2+3s), c_4 = -(s+1)(2s+1)(7s+5)$ . Further, for  $s = 1$  the sequence is [38, A177384], for  $s = 2$  it is [38, A064037]. The case  $s = -3$  produces

$$(7.6) \quad \gamma(\alpha) = -\alpha + 2\alpha^2 - 14\alpha^3 + 160\alpha^4 - 2444\alpha^5 + 45792\alpha^6 - 1005480\alpha^7 + 25169760\alpha^8 \mp \dots$$

Compare this to [6, Table 1], in which  $G(\alpha, x)$  is inserted into both the internal edges of the primitive. Our result eq. (7.6) reproduces the purely rational part of the latter, but not the terms proportional to  $\zeta(j)$ .

The anomalous dimension considered so far,  $\gamma(\alpha) =: \gamma^{\text{pert}}(\alpha)$ , is the perturbative solution to the differential equation 2.18,

$$(7.7) \quad -(1 + \gamma(\alpha)(s\alpha\partial_\alpha + 1))\gamma(\alpha) = \alpha.$$

This ODE has also non-perturbative solutions [9, 11] of the form

$$(7.8) \quad \gamma^{\text{non-pert}}(\alpha) = \alpha^\beta \exp\left(-\frac{\lambda}{\alpha}\right) \left(1 + b^{(1)}\alpha + b^{(2)}\alpha^2 + \dots\right).$$

We use the method of [9, V. A.] to determine the unknown coefficients<sup>1</sup>. The ansatz  $\gamma(\alpha) = \gamma^{\text{pert}}(\alpha) + \gamma^{\text{non-pert}}(\alpha)$  is inserted into eq. (7.7) and the above coefficients  $c_j$  are used for  $\gamma^{\text{pert}}$ . The equation is then linearized in  $\gamma^{\text{non-pert}}$ . The resulting series in  $\alpha$  has to vanish, this leads to the expressions listed in eq. (D.1), especially  $\lambda(s) = 1/s, \beta(s) = -(3+2s)/s$ . For  $s = -2$  we reproduce [11, (25)] up to different sign conventions regarding  $\alpha$ , mentioned below eq. (7.2).

The coefficients  $c_n$  of the perturbative solution of the non-linear DSE eq. (7.7), grow factorially, which has been studied repeatedly [10, 11, 13, 7]. The asymptotic behaviour of  $c_n$  is dictated by the non-perturbative solution eq. (7.8), [3] (alternatively, use the methods of [7]), namely for  $n \rightarrow \infty$

$$(7.9) \quad c_n \sim S(s) \cdot \frac{1}{\lambda(s)^n} \cdot \Gamma(n - \beta(s)) \left(1 + \frac{\lambda(s) \cdot b^{(1)}(s)}{(n - \beta(s) - 1)} + \frac{\lambda(s)^2 \cdot b^{(2)}(s)}{(n - \beta(s) - 1)(n - \beta(s) - 2)} + \dots\right).$$

We computed 500 series coefficients of  $\gamma^{\text{pert}}(\alpha)$  and extracted their asymptotic behaviour using order-70 Richardson extrapolation. This produced at least 50 significant digits and confirmed the expressions  $\lambda(s), \beta(s), b^{(1)}(s), b^{(2)}(s)$  and  $b^{(3)}(s)$  listed in eq. (D.1). The Stokes constant  $S(s)$  is reported in table 7. One recognizes [11],  $S(-2) = 1/(\sqrt{\pi}e)$  and also  $S(-3) = 3/(\pi e^2)$ , all other Stokes constants appear unfamiliar<sup>2</sup>.

To visualize the asymptotic behaviour, we consider the ratio

$$(7.10) \quad \frac{c_{n+1}/\Gamma(n+1-\beta(s))}{c_n/\Gamma(n-\beta(s))} \equiv \frac{c_{n+1}}{(n + \frac{3+2s}{s})c_n} = s - b^{(1)}(s)\frac{1}{n^2} + \mathcal{O}\left(\frac{1}{n^3}\right) \quad (\text{for } s \neq 0, -1).$$

There is no  $1/n$  correction to this quantity, hence it converges quickly, as shown in Figure 4 (A).

The shift from MOM- to MS-bar-renormalization is computed as discussed in section 3.1. The first coefficients are reported in table 8, for example, for  $s = -2$  one obtains

$$\begin{aligned} \bar{\gamma}_0(\alpha) &= 1 + 2\alpha - \frac{11}{2}\alpha^2 + \frac{88}{3}\alpha^3 - \left(\frac{1781}{8} + \frac{\zeta(3)}{3}\right)\alpha^4 + \left(\frac{42613}{20} + \frac{\pi^2}{150} - \frac{12\zeta(3)}{5}\right)\alpha^5 - \mathcal{O}(\alpha^6) \\ \ln \bar{\delta}(\alpha) &= -2 + \frac{3}{2}\alpha - \frac{29}{6}\alpha^2 + \frac{94 - \zeta(3)}{3}\alpha^3 - \left(\frac{5573}{20} + \frac{\pi^4}{150} - \frac{7\zeta(3)}{5}\right)\alpha^4 \mp \dots \end{aligned}$$

<sup>1</sup>The author thanks Gerald Dunne for suggesting the method.

<sup>2</sup>The Stokes constant  $S(s)$  was also computed for non-integer  $s$ . It appears to be a fairly smooth function of  $s$ , with zeros, as expected, at the points  $s = -1$  and  $s = 0$ . Remarkably, inside the interval  $(-1, 0)$  the function is oscillating and has additional zeros, accumulating near  $s = 0$ . This could be worth further study.

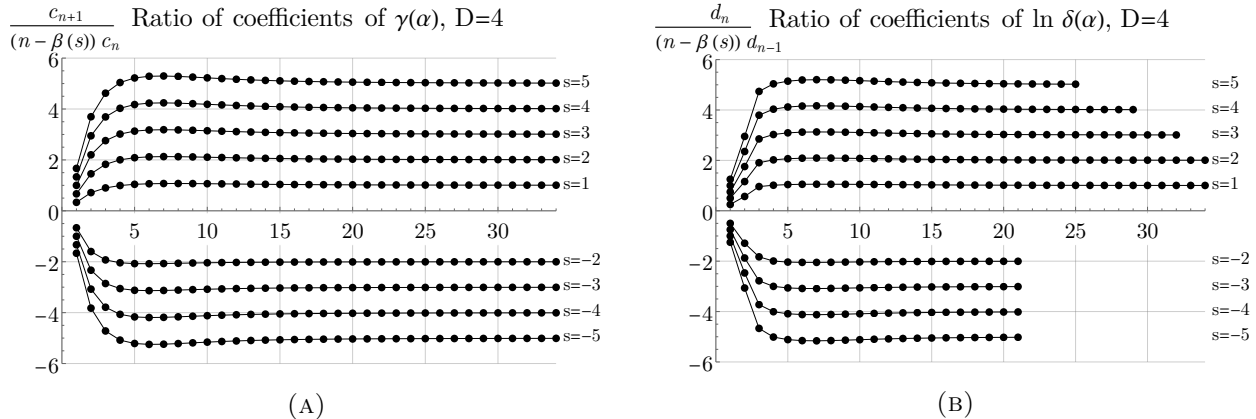


FIGURE 4. (A) Ratio of successive coefficients  $c_n$  of  $\gamma(\alpha) = \sum c_n \alpha^n$  for the physical model in  $D = 4$  dimensions. The denominator  $(n - \beta(s))$  is chosen to match the known asymptotics eq. (7.9). The ratio quickly converges towards the limit  $s$ , see eq. (7.10). (B) Ratio of successive coefficients  $d_n$  of  $\ln \delta(\alpha) = \sum_n d_n \alpha^n$ . Seemingly, it converges to the same limit  $s$  as the ratio in (A). The computation is much harder for negative  $s$ , therefore only a lower order  $n$  is available.

We write  $\ln \bar{\delta}(\alpha) = \sum d_n \alpha^n$ , where the coefficients  $d_n$  were computed up to order  $\alpha^{10}$  symbolically and to at least order  $\alpha^{20}$  numerically. As expected from eq. (3.11), the constant coefficient is  $d_0 = -2$  for all  $s$ . Similarly to eq. (7.10), we examine the ratio of successive  $d_n$ , the result is shown in fig. 4 (B). We extract numerical estimates for the growth parameters in the ansatz

$$(7.11) \quad d_n \sim \tilde{S}(s) \cdot \tilde{F}(s)^n \cdot \Gamma(n - \tilde{\beta}(s)) \left( 1 + \frac{\tilde{b}^{(1)}(s)}{(n - \tilde{\beta}(s) - 1)} + \dots \right)$$

by the following method: We use Richardson extrapolation[36, 3] of orders 2,3,4 and 5 and take their mean as the estimation and the largest absolute difference between any of these as uncertainty. Experiments with the coefficients  $c_n$  of  $\gamma(\alpha)$  show that this procedure likely overestimates the uncertainties.

| $s$ | $n_{\max}$ | $\tilde{S}(s)/s$       | $\tilde{F}(s)$     | $\tilde{\beta}(s)$ | $\tilde{b}^{(1)}(s)$ |
|-----|------------|------------------------|--------------------|--------------------|----------------------|
| 5   | 24         | $-0.02532 \pm 0.00037$ | $4.987 \pm 0.062$  | $-3.59 \pm 0.12$   | $-2.61 \pm 0.18$     |
| 4   | 27         | $-0.02709 \pm 0.00019$ | $3.993 \pm 0.036$  | $-3.74 \pm 0.08$   | $-2.79 \pm 0.11$     |
| 3   | 32         | $-0.02749 \pm 0.00011$ | $2.997 \pm 0.017$  | $-3.99 \pm 0.04$   | $-3.10 \pm 0.06$     |
| 2   | 38         | $-0.02272 \pm 0.00010$ | $1.999 \pm 0.009$  | $-4.50 \pm 0.03$   | $-3.74 \pm 0.05$     |
| 1   | 38         | $-0.00541 \pm 0.00009$ | $0.999 \pm 0.007$  | $-6.00 \pm 0.04$   | $-5.97 \pm 0.12$     |
| -2  | 21         | $0.2080 \pm 0.0018$    | $-1.998 \pm 0.012$ | $-1.49 \pm 0.05$   | $-0.74 \pm 0.08$     |
| -3  | 21         | $0.1295 \pm 0.0014$    | $-2.995 \pm 0.026$ | $-1.99 \pm 0.07$   | $-1.10 \pm 0.11$     |
| -4  | 21         | $0.0882 \pm 0.0011$    | $-3.993 \pm 0.040$ | $-2.24 \pm 0.09$   | $-1.30 \pm 0.14$     |
| -5  | 21         | $0.0655 \pm 0.0009$    | $-4.991 \pm 0.054$ | $-2.40 \pm 0.10$   | $-1.43 \pm 0.15$     |

TABLE 1. Numerical findings of the growth parameters of  $\ln \bar{\delta}(\alpha)$  in the  $D = 4$  model section 7, according to eq. (7.11). They are consistent with table 7 and eq. (D.1).  $\ln \bar{\delta}(\alpha)$  was computed including order  $\alpha^{n_{\max}}$ .

The results are reported in table 1. They are consistent with  $\tilde{S}(s) = s \cdot S(s)$ ,  $\tilde{F}(s) = s$  and  $\tilde{\beta}(s) = \beta(s) - 1$  within around 1% relative uncertainty. Unlike the above analysis of  $\gamma$ , at this

level of uncertainty our findings of “rational numbers” are to be understood as educated guesswork rather than proofs. The estimates obtained for  $\tilde{b}^{(1)}(s)$  are too imprecise to deduce a formula at this point.

It turns out to be very useful to compare the coefficients of  $\ln \delta(\alpha)$  to those of  $\gamma(\alpha)$ . To this end we compute the ratio  $d_n/(s\lambda c_{n+1})$ , where  $s \cdot \lambda(s) = 1$  in our case. Using eq. (7.11) with table 1, we expect that  $d_n/c_{n+1} \rightarrow 1$ . As before, we use Richardson extrapolation of order 2,3,4 and 5 to determine the parameters in

$$(7.12) \quad \frac{d_n}{s\lambda c_{n+1}} \sim r(s) + r_1(s)\frac{1}{n} + r_2(s)\frac{1}{n^2} + \dots, \quad n \rightarrow \infty.$$

| $s$ | $r_1(s)$              | $r_2(s)$            | $r_3(s)$          | $r_4(s)$        | $r_5(s)$        |
|-----|-----------------------|---------------------|-------------------|-----------------|-----------------|
| 5   | $1.20002 \pm 0.00012$ | $0.0003 \pm 0.0019$ | $0.005 \pm 0.031$ | $0.09 \pm 0.50$ | $1.3 \pm 7.9$   |
| 4   | $1.25000 \pm 0.00001$ | $0.0000 \pm 0.0002$ | $0.000 \pm 0.003$ | $0.01 \pm 0.05$ | $0.18 \pm 0.95$ |
| 3   | $1.33333 \pm 0.00001$ | $0.0000 \pm 0.0001$ | $0.000 \pm 0.001$ | $0.01 \pm 0.01$ | $0.00 \pm 0.02$ |
| 2   | $1.50000 \pm 0.00001$ | $0.0000 \pm 0.0001$ | $0.000 \pm 0.001$ | $0.00 \pm 0.01$ | $0.00 \pm 0.01$ |
| 1   | $2.00000 \pm 0.00001$ | $0.0000 \pm 0.0001$ | $0.000 \pm 0.001$ | $0.00 \pm 0.01$ | $0.00 \pm 0.01$ |
| -2  | $0.50000 \pm 0.00001$ | $0.0000 \pm 0.0001$ | $0.000 \pm 0.001$ | $0.00 \pm 0.01$ | $0.00 \pm 0.02$ |
| -3  | $0.66667 \pm 0.00001$ | $0.0000 \pm 0.0002$ | $0.000 \pm 0.002$ | $0.01 \pm 0.03$ | $0.07 \pm 0.39$ |
| -4  | $0.75001 \pm 0.00004$ | $0.0001 \pm 0.0005$ | $0.001 \pm 0.007$ | $0.02 \pm 0.09$ | $0.20 \pm 1.24$ |
| -5  | $0.80001 \pm 0.00006$ | $0.0002 \pm 0.0009$ | $0.002 \pm 0.012$ | $0.03 \pm 0.17$ | $0.4 \pm 2.3$   |

TABLE 2. Parameters of the ratio  $d_n/c_{n+1}$  for  $D = 4$  from eq. (7.12).  $r_{\geq 2}$  is consistent with zero.

We find  $r(s) = 1$  with uncertainty smaller  $10^{-5}$ . The numerical results for the corrections  $r_j(s)$  are reported in table 2. The relative uncertainties are much smaller than for the above parameters of eq. (7.11). They suggest the simple formula  $r(s) = 1$  and  $r_1(s) = (s + 1)/s$ . Inserting this, surprisingly, the higher order corrections  $r_{j \geq 2}(s)$  seem to vanish.

Together with the known behaviour of  $c_{n+1}$ , eq. (7.9) and  $\beta(s) = -(3 + 2s)/s$ , we conclude

$$(7.13) \quad d_n \sim S(s)s^{n+1}\Gamma(n - \beta(s) + 1) \left( 1 + \frac{-1+3s+2s^2}{s^2} + \frac{1+4s+4s^2-6s^3-7s^4}{2s^4} + \mathcal{O}\left(\frac{1}{n^3}\right) \right).$$

The subleading coefficient is consistent with the value  $\tilde{b}^{(1)}(s)$  which we found in table 1.

For the higher order corrections in table 2, the uncertainties are increasing. If we nonetheless speculate that their vanishing is a general pattern, then we obtain

$$(7.14) \quad d_n = \left( 1 + \frac{s+1}{sn} \right) \cdot c_{n+1} + e_n.$$

The numerical values suggest that the remainder  $e_n$  falls off factorially, see fig. 6 (A). Using the ring of factorially divergent power series[10], this asymptotic statement can be translated to a relation between the corresponding generating functions<sup>3</sup>:

$$(7.15) \quad \ln \bar{\delta}(\alpha) = \frac{\gamma(\alpha)}{\alpha} + \frac{s+1}{s} \int \frac{d\alpha}{\alpha} \frac{\gamma(\alpha)}{\alpha} + f(\alpha), \quad s \neq 0.$$

Figure 6 (B) shows the coefficients of the function  $f(\alpha) := \sum_{n=1}^{\infty} f_n \alpha^n$ , they seemingly grow exponentially, not factorially. This indicates that  $f(\alpha)$  is a convergent power series around  $\alpha = 0$ . The growth rate is reported in table 8. The coefficients of the function  $f(\alpha)$  contain zeta values, which appear in  $\ln \bar{\delta}(\alpha)$  but not in  $\gamma(\alpha)$ . The author has not succeeded in finding a closed formula.

<sup>3</sup>The author thanks Michael Borinsky for pointing this out.

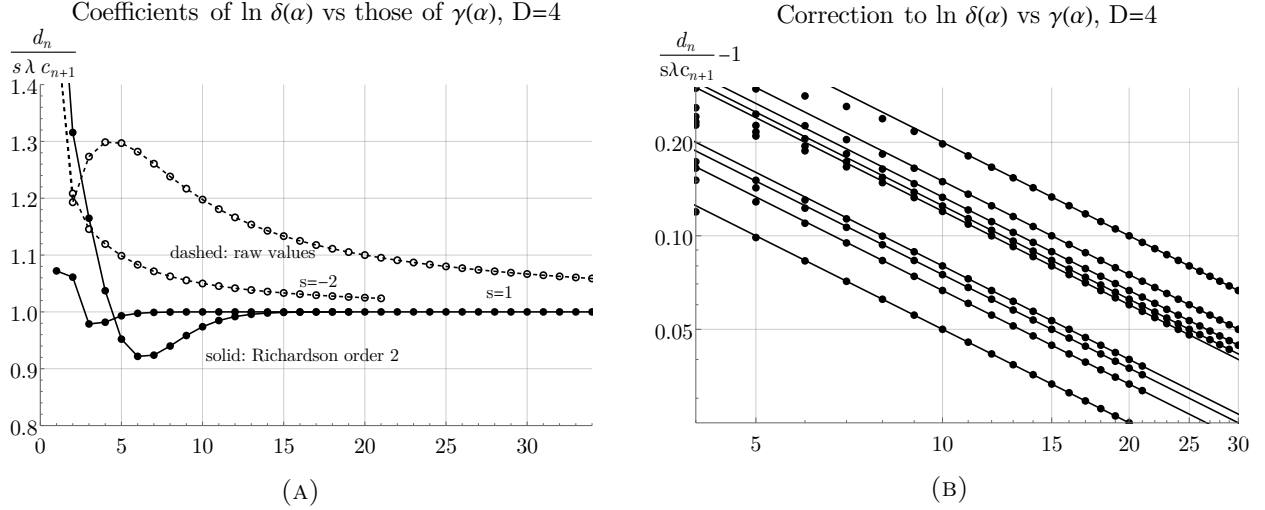


FIGURE 5. (A) Ratio of the coefficients of  $\ln \delta(\alpha) = \sum d_n \alpha^n$  and  $\gamma(\alpha) = \sum c_n \alpha^n$ . Shown are two representative sequences, namely  $s = -2$  and  $s = 1$ . For each of them, the dashed line indicates the raw values while the solid line is the order-2 Richardson extrapolation. The ratio  $d_n/c_{n+1}$  approaches the limit unity. (B) Correction to this ratio. The points are the values of  $\frac{d_n}{c_{n+1}} - 1$  for the different  $s$ . Solid lines are the functions  $\frac{s+1}{sn}$ , they match the points surprisingly well even for low orders. The remaining difference falls off faster than  $1/n^2$ .

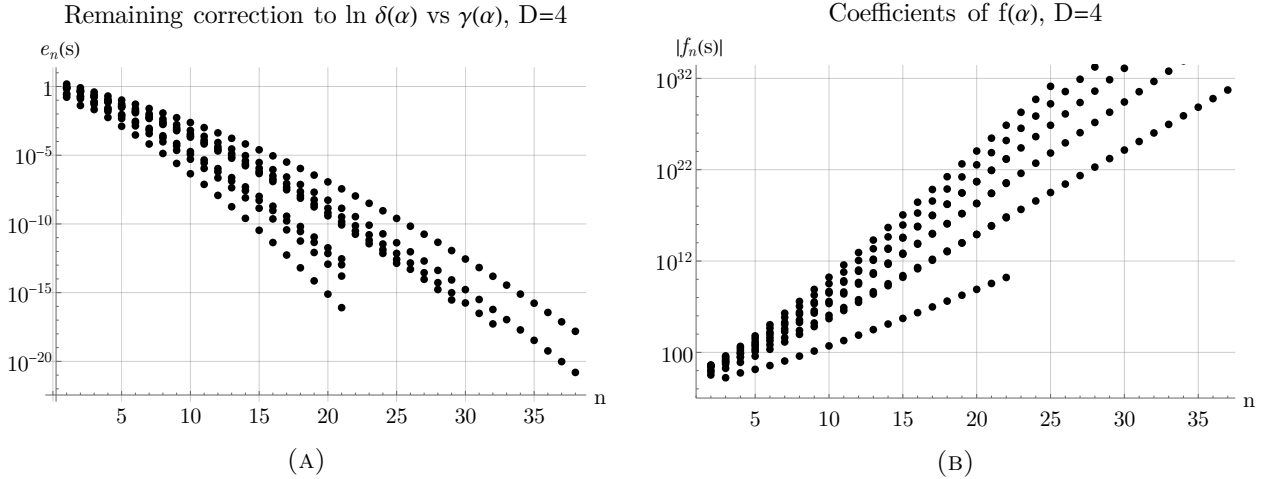


FIGURE 6. (A) Remainder coefficients  $e_n$  from eq. (7.14), for the different values of  $s$ . This is a logarithmic plot, they decay faster than exponentially. (B) Coefficients of the function  $f(\alpha)$  in eq. (7.15). The data points overlap for different  $s$ . The coefficients grow exponentially, which suggests that  $f(\alpha)$  is an analytic function.

## 8. NON-LINEAR DSE IN $D = 6$

Following the procedure of section 7.1, we also evaluate the 6-dimensional model of section 5 for various powers  $s \in \{-5, \dots, +5\}$  in the invariant charge eq. (7.1).

The leading-log functions  $H_1, H_2, H_3$  are as expected from eq. (2.20). The anomalous dimension  $\gamma(\alpha)$  contains only rational coefficients for all values of  $s$ . Up to the computed symbolic precision  $\alpha^{12}$ , they fulfil the ODE eq. (2.18), which here takes the form

$$(8.1) \quad (3 + \gamma(s\alpha\partial_\alpha + 1))(2 + \gamma(s\alpha\partial_\alpha + 1))(1 + \gamma(s\alpha\partial_\alpha + 1))\gamma = \alpha.$$

The perturbative solution  $\gamma^{\text{pert}}(\alpha) = \sum_{j=0}^{\infty} c_j \alpha^j$  can be computed to high order from this ODE, the first coefficients are

$$c_1 = \frac{1}{6}, \quad c_2 = -\frac{11(s+1)}{216}, \quad c_3 = \frac{(s+1)(206+291s)}{7776}, \quad c_4 = -\frac{(s+1)(4711+14887s+11326s^2)}{279936}.$$

We use these coefficients, insert the non-perturbative ansatz eq. (7.8) into eq. (8.1), linearize, and solve for the parameters  $\beta, \lambda, b^{(1)}, b^{(2)}, b^{(3)}$ . Equation (8.1) is of third order, unlike in the case  $D=4$ , we find three linearly independent solutions eq. (D.2). In the ansatz eq. (7.8), the solution with smallest absolute  $\lambda$  is dominant, this is the first entry of the vectors eq. (D.2).

With these parameters, the series coefficients  $c_n$  of the perturbative solution grow according to eq. (7.9). We have confirmed this behaviour numerically from the first 500 coefficients  $c_n$  for  $s \in \{-5, \dots, +5\}$ . The Stokes constant  $S(s)$  is reported in table 9, we reproduce the value [9, (15)] for  $s = -2$ . Like eq. (7.10), the ratio of successive coefficients  $c_{n+1}/((n - \beta_1(s))c_n)$  is constant up to quadratic corrections.

The power series coefficients of the shift  $\ln \hat{\delta}(\alpha)$  have been computed symbolically up to order  $\alpha^{10}$ , the leading ones are reported in table 10. The numerical computation extends further, depending on  $s$ . The ratio of successive coefficients, with the same normalization as for  $\gamma(\alpha)$ , is shown in fig. 7(A). The plot suggests that  $c_n$  grow at a similar rate as  $d_n$ .

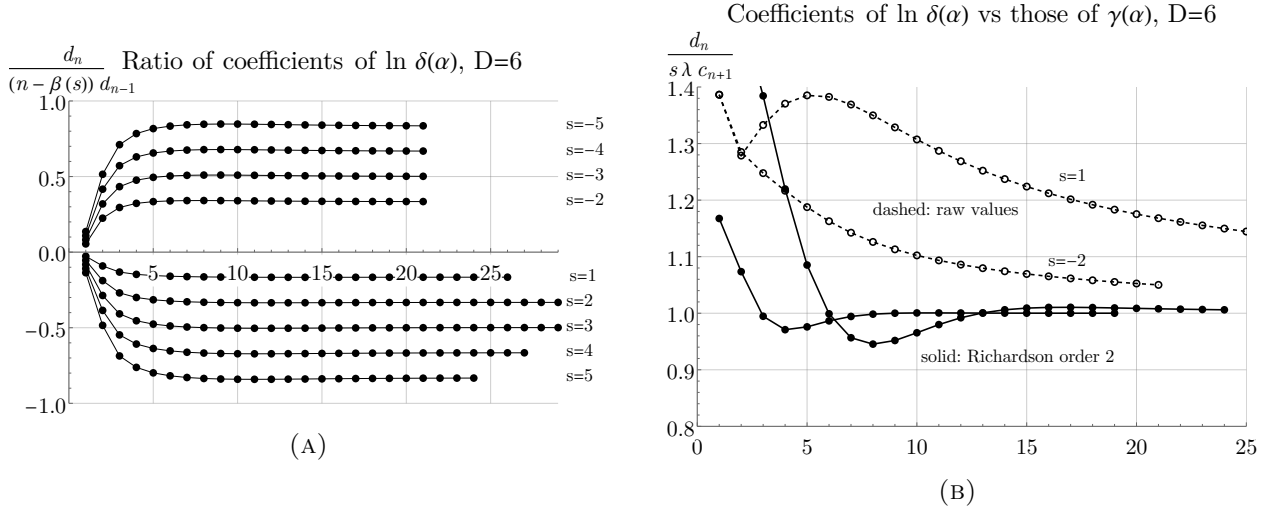


FIGURE 7. (A) Ratio of successive coefficients  $d_n$  of  $\ln \delta(\alpha)$ , divided by the assumed leading asymptotic behaviour from eq. (D.2), for  $D = 6$ . This quantity quickly approaches the limit  $-s/6$ . (B) Ratio between the coefficients  $d_n$  of  $\ln \delta(\alpha)$  and the coefficients  $c_{n+1}$  of  $\gamma(\alpha)$ . Compared to fig. 5 (A), the Richardson extrapolation converges slower, indicating a significant  $1/n^2$ -correction, see table 4.

As explained in section 7.2, we extracted numerical estimates of the parameters in eq. (7.11). They are given in table 3 and are consistent with  $\tilde{S}(s) = s \cdot S(s)$ ,  $\tilde{F}(s) = -s/6$  and  $\tilde{\beta}(s) = \beta_1(s) - 1$ . Once more, the relative uncertainty of about 1% of these values is too large to rigorously identify the rational values.

| $s$ | $n_{\max}$ | $10^6 \cdot \bar{S}(s)/s$ | $\bar{F}(s)$       | $\bar{\beta}(s)$  |
|-----|------------|---------------------------|--------------------|-------------------|
| 5   | 24         | $-50.1 \pm 4.5$           | $-0.833 \pm 0.018$ | $-7.00 \pm 0.37$  |
| 4   | 27         | $-34.5 \pm 2.4$           | $-0.666 \pm 0.012$ | $-7.25 \pm 0.23$  |
| 3   | 29         | $-16.6 \pm 1.2$           | $-0.500 \pm 0.007$ | $-7.72 \pm 0.19$  |
| 2   | 29         | $-2.97 \pm 0.28$          | $-0.333 \pm 0.006$ | $-8.68 \pm 0.26$  |
| 1   | 26         | $-0.0054 \pm 0.0015$      | $-0.167 \pm 0.006$ | $-11.64 \pm 0.75$ |
| -2  | 21         | $87900 \pm 1600$          | $0.333 \pm 0.005$  | $-2.92 \pm 0.12$  |
| -3  | 21         | $18000 \pm 560$           | $0.500 \pm 0.009$  | $-3.90 \pm 0.21$  |
| -4  | 21         | $6690 \pm 290$            | $0.666 \pm 0.013$  | $-4.39 \pm 0.26$  |
| -5  | 21         | $3410 \pm 180$            | $0.833 \pm 0.018$  | $-4.69 \pm 0.29$  |

TABLE 3. Numerical findings of the growth parameters of  $\ln \bar{\delta}(\alpha)$  in the  $D = 6$  model section 8, according to eq. (7.11). They are consistent with table 9 and eq. (D.2).

| $s$ | $r(s)$              | $r_1(s)$          | $r_2(s)$         |
|-----|---------------------|-------------------|------------------|
| 5   | $1.0010 \pm 0.0017$ | $2.573 \pm 0.072$ | $-6.91 \pm 0.84$ |
| 4   | $1.0007 \pm 0.0019$ | $2.685 \pm 0.072$ | $-7.3 \pm 1.4$   |
| 3   | $1.0007 \pm 0.0024$ | $2.863 \pm 0.078$ | $-8.4 \pm 1.8$   |
| 2   | $1.0010 \pm 0.0026$ | $3.21 \pm 0.11$   | $-11.2 \pm 1.8$  |
| 1   | $1.0032 \pm 0.0048$ | $4.22 \pm 0.23$   | $-22.3 \pm 1.3$  |
| -2  | $1.0000 \pm 0.0002$ | $1.083 \pm 0.003$ | $-1.10 \pm 0.34$ |
| -3  | $1.0002 \pm 0.0004$ | $1.441 \pm 0.012$ | $-1.80 \pm 0.07$ |
| -4  | $1.0003 \pm 0.0007$ | $1.619 \pm 0.018$ | $-2.33 \pm 0.16$ |
| -5  | $1.0004 \pm 0.0008$ | $1.726 \pm 0.022$ | $-2.71 \pm 0.22$ |

TABLE 4. Parameters of the ratio  $d_n/(-6c_{n+1})$  for  $D = 6$  from eq. (7.12).

The ratio  $d_n/(s\lambda c_{n+1}) = d_n/(-6c_{n+1})$  is depicted in fig. 7 (B) for two values of  $s$ . The asymptotic parameters, according to eq. (7.12), are given in table 4. Unlike for  $D = 4$ , this ratio does not converge particularly quickly. A fit suggests that  $r_1(s) = (2.12 + 2.15s)/s$ , but the uncertainties are too large to identify the numbers as rational. This is reflected by the large absolute values we obtain for the  $1/n^2$ -correction  $r_2(s)$ , see table 4. In  $D = 4$ , this correction vanished and therefore allowed us to extract  $r_1(s)$  precisely.

All in all, we can not clearly identify the subleading corrections of  $d_n$  in the  $D = 6$  model, but the findings at least suggest that the leading growth coincides with the one of  $c_{n+1}$ , that is

$$(8.2) \quad d_n \sim S(s)s \left(-\frac{s}{6}\right)^n \Gamma\left(n+1 + \frac{35+29s}{6s}\right).$$

## 9. NON-LINEAR TOY MODEL

We solved the DSE for  $s \in \{-5, \dots, +4\}$  symbolically to order  $\alpha^{16}$ . The leading-log functions  $H_1, H_2$  and  $H_3$  agree with the general formula eq. (2.20) of [31] for the appropriate choice  $g_1 = 1, g_2 = 0, g_3 = \pi^2/2$  and for all values of  $s$ . Especially, for  $s = -2$ , we confirm  $H_1$  from [35, Cor. 3.6.4] and  $H_2 = H_4 = H_6 = 0$ .

The symbolic results for the anomalous dimension fulfil eq. (2.18),

$$(9.1) \quad -\frac{\sin(u)}{u} \Big|_{u \rightarrow -\gamma(1+s\alpha\partial_\alpha)} \gamma(\alpha) = \alpha.$$

Unlike eqs. (7.7) and (8.1), the ODE eq. (9.1) of the toy model is of infinite order. This is in interesting contrast to the comparatively simple integral kernel coefficients eq. (B.4) of the toy model.

We computed a symbolic perturbative power series solution  $\gamma(\alpha) = \sum c_n \alpha^n$  of eq. (9.1) to order 450 and extracted the asymptotic behaviour. The result has the form eq. (7.9) for  $n$  odd. We find  $\beta(s) = -(2+s)/s$ , numerical values of the constants  $S(s)$ ,  $b^{(1)}(s)$  and  $b^{(2)}(s)$  are given in table 11. We did not recognize these numbers apart from the Stokes constant  $S(-2) = 2/\pi$ .

By eq. (3.11), the shift  $\ln \delta(\alpha) = \sum d_n \alpha^n$  does not have a constant term in the toy model. The first coefficients for the shift are reported in table 12, while table 5 contains the numerical estimates for the growth parameters.

| $s$ | $n_{\max}$ | $\tilde{S}(s)/s$    | $\tilde{F}(s)$    | $\tilde{\beta}(s)$ |
|-----|------------|---------------------|-------------------|--------------------|
| 4   | 23         | $-0.389 \pm 0.010$  | $3.985 \pm 0.081$ | $-2.50 \pm 0.21$   |
| 3   | 23         | $-0.485 \pm 0.015$  | $2.988 \pm 0.068$ | $-2.68 \pm 0.24$   |
| 2   | 23         | $-0.612 \pm 0.023$  | $1.991 \pm 0.059$ | $-3.02 \pm 0.31$   |
| 1   | 23         | $-0.572 \pm 0.037$  | $0.996 \pm 0.056$ | $-4.09 \pm 0.56$   |
| -2  | 23         | $0.6382 \pm 0.0067$ | $1.997 \pm 0.012$ | $-0.991 \pm 0.050$ |
| -3  | 23         | $0.5275 \pm 0.0076$ | $2.994 \pm 0.024$ | $-1.322 \pm 0.071$ |
| -4  | 23         | $0.4202 \pm 0.0069$ | $3.991 \pm 0.037$ | $-1.488 \pm 0.082$ |
| -5  | 23         | $0.3443 \pm 0.0060$ | $4.988 \pm 0.051$ | $-1.588 \pm 0.088$ |

TABLE 5. Numerical findings of the growth parameters of  $\ln \bar{\delta}(\alpha)$  in the toy model, according to eq. (7.11).  $\tilde{S}(s)$  is consistent with table 11.

The toy model has the property that both  $c_n$  and  $d_n$  vanish for even  $n$ . This is problematic for two reasons: Firstly, although we computed numerically the order  $\alpha^{23}$ , we only get 12 non-vanishing coefficients of  $\ln \delta(\alpha)$ . Secondly, we can not compute the ratio  $d_n/c_{n+1}$  and therefore not use the trick which allowed us to extract the behaviour of  $d_n$  in the  $D = 4$  physical model section 7.

To visualize the coefficients  $d_n$  of  $\ln \delta(\alpha)$ , we consider the following two ratios for odd  $n$ :

$$(9.2) \quad R^{(\delta)} := \sqrt{\frac{d_{n+2}}{(n - \beta(s) + 1)(n - \beta(s) + 2)d_n}}, \quad R^{(\delta/\gamma)} := \frac{d_n}{s \cdot (n - \beta(s) + 1)c_n}.$$

Figure 8 (A) shows that  $R^{(\delta)}$  approaches the limit  $|s|$ , which suggests that  $d_n$  scale asymptotically  $\sim s^n \Gamma(n - \beta(s) + 1)$ , with (approximately) the same  $\beta(s)$  as the coefficients  $c_n$  of  $\gamma(\alpha)$ . The quantity  $R^{(\delta/\gamma)}$  allows to fix the Stokes constant, it is shown in fig. 8 (B). The limit of  $R^{(\delta/\gamma)}$  is  $1.00 \pm 0.02$ , suggesting that the Stokes constant agrees with the one of  $\gamma(\alpha)$ . In table 5, the direct estimates of the asymptotic growth are reported. All in all, it seems that the coefficients of  $\ln \delta(\alpha)$  grow factorially according to

$$(9.3) \quad d_n \sim S(s) s^{n+1} \Gamma(n + (2 + 2s)/s).$$

We did not try to determine subleading corrections.

**9.1. Exact solution of the case  $s=-2$ .** We end this paper with a curious empirical observation. For  $s = -2$ , at least up to  $\mathcal{O}(\alpha^{18})$ , the perturbative anomalous dimension in MS turns out to be the same one as for a non-iterative DSE  $s = -1$ , namely

$$\bar{\gamma}(\alpha) = -\alpha \quad \text{for } s = -1 \text{ and } s = -2.$$

Equivalently, the MS counter term for  $s = -2$  takes the same form as the leading log Green function eq. (2.20),  $\bar{Z}(\alpha, \epsilon) = \sqrt{1 - 2\alpha/\epsilon} + \mathcal{O}(\alpha^{18})$ . One can conjecture that this holds for all orders in perturbation theory.

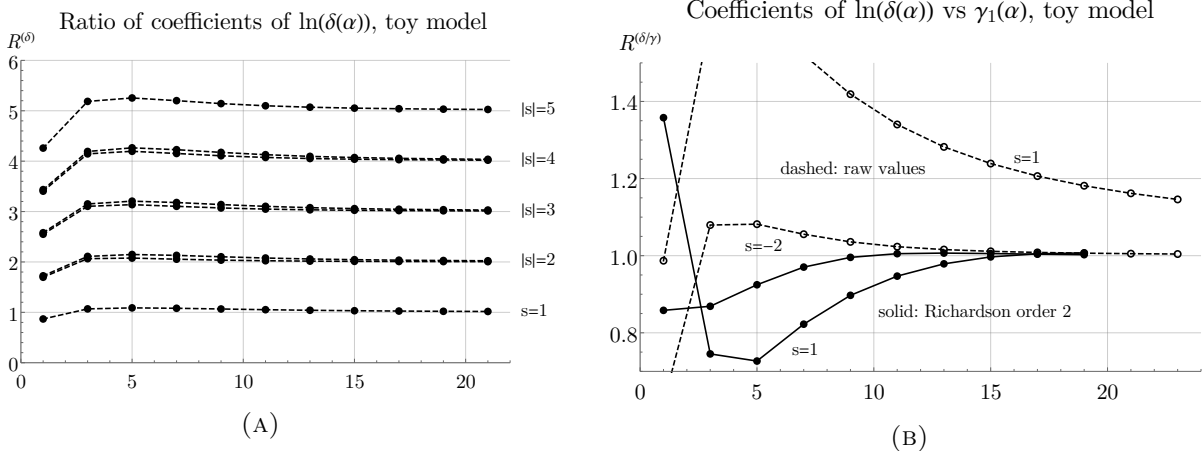


FIGURE 8. (A) Ratio eq. (9.2) of successive coefficients of  $\ln \delta(\alpha)$ . The ratio visibly approaches  $|s|$ , Richardson extrapolation (not shown) confirms this. (B) Ratio  $R^{(\delta/\gamma)}$  between coefficients of  $\ln \delta(\alpha)$  and  $\gamma(\alpha)$  and its order-2-Richardson extrapolation. The limit seems to be unity, but knowing only 12 terms the uncertainty is large. Compare the first 12 terms of fig. 5 (A).

In both cases, the anomalous dimension  $\bar{\gamma}(\alpha) = -\alpha$  leads to a simple Callan-Symanzik-equation eq. (2.13) which can be solved explicitly. In the trivial case  $s = -1$  the beta function is  $\bar{\beta}(\alpha) = \alpha$ ,

$$-\alpha \bar{G}(\alpha, \bar{x}) + \alpha^2 \partial_\alpha \bar{G}(\alpha, \bar{x}) = \bar{x} \partial_{\bar{x}} \bar{G}(\alpha, \bar{x}) \quad \Rightarrow \quad \bar{G}(\alpha, \bar{x}) = K(1 + \alpha \ln \bar{x}), \quad K \in \mathbb{C}.$$

The constant  $K = 1$  can be fixed by an obvious matching with the perturbative solution. For  $s = -2$  we have  $\bar{\beta}(\alpha) = 2\alpha$  and the partial differential equation eq. (2.13),

$$-\alpha \bar{G}(\alpha, \bar{x}) + 2\alpha^2 \partial_\alpha \bar{G}(\alpha, \bar{x}) = \bar{x} \partial_{\bar{x}} \bar{G}(\alpha, \bar{x}),$$

has the general solution

$$(9.4) \quad \bar{G}(\alpha, \bar{x}) = \frac{C}{\sqrt{\alpha}} - 2C\sqrt{\alpha} \ln \bar{x}, \quad C \in \mathbb{C}.$$

Using eq. (3.1), this amounts to the MOM Green function  $G(\alpha, x) = \bar{G}(\alpha, \delta^{-1}x)$ . From the renormalization condition eq. (2.12) one concludes that  $\ln \delta(\alpha) = \frac{1}{2C\sqrt{\alpha}} - \frac{1}{2\alpha}$ . Hence the MOM Green function and MOM anomalous dimension are

$$(9.5) \quad G(\alpha, x) = 1 - 2C\sqrt{\alpha} \ln x, \quad \gamma(\alpha) = -2C\sqrt{\alpha}.$$

Note that the multiplicative shift factor  $\delta(\alpha) = e^{\ln \delta(\alpha)}$  vanishes in the limit  $\alpha \rightarrow 0$  and the MS-bar Green function eq. (9.4) diverges while the MOM function eq. (9.5) does not.

The MOM anomalous dimension from eq. (9.5) fulfils  $(1 - 2\alpha \partial_\alpha) \gamma(\alpha) = 0$  and hence all higher anomalous dimensions  $\gamma_{k \geq 2}(\alpha)$  from eq. (2.16) vanish in accordance with eq. (2.15). On the other hand,  $\gamma(\alpha) = -2C\sqrt{\alpha}$  violates the infinite-order “differential equation” 9.1. The function  $\gamma(\alpha)$  is not analytic at the origin  $\alpha = 0$ . It remains a task for future study to clarify if the differential equation eq. (2.18) holds for non-perturbative solutions  $\gamma(\alpha)$  at all, and what its significance is in the case where it involves infinitely many derivatives and therefore, naively, infinitely many free integration constants.

## 10. CONCLUSION

We have discussed how a Green function in Minimal Subtraction (MS) is related to its corresponding Green function in kinematic renormalization (MOM). To this end, we have examined and used various relations between the renormalization group functions and  $Z$ -factors to find the shift of the renormalization point (section 3). We have then applied this procedure to propagator-type Dyson-Schwinger equations with three different kernels. For various relevant quantities, we have computed their series coefficients symbolically and numerically and sometimes identified the coefficients' algebraic formulas. In all cases where there is an overlap, our results agree with the ones reported in earlier literature. The key outcomes of the present work are:

- (1) It is possible to match the Green functions of MS, MS-bar and MOM schemes to all orders in perturbation theory, in the limit  $\epsilon \rightarrow 0$ , if a suitable kinematic renormalization point  $\delta(\alpha) \cdot \mu$  is chosen, where  $\mu$  is the mass scale of dimensional regularization, see section 3.1.
- (2) In the linear examples, the factors  $\delta(\alpha)$  between the renormalization points have been deduced in closed form as  $\delta(\alpha) = \gamma_0^{1/\gamma}$ , see eqs. (4.15), (5.1) and (6.2). The result is finite in perturbation theory and proportional to  $\sqrt{\partial_\alpha \gamma(\alpha)}$ . It also encodes information about the MOM-solution for  $\epsilon \neq 0$ , see eq. (3.7).
- (3) For non-linear DSEs, series coefficients for  $\gamma(\alpha)$  and  $\ln \delta(\alpha)$  have been computed for several different exponents  $s$  in the invariant charge  $Q = G^s$ . The results are highly regular in  $s$ . The first symbolic coefficients of  $\ln \delta(\alpha)$  are collected in appendix E.
- (4) The coefficients  $d_n$  of  $\ln \delta(\alpha)$  seem to grow factorially. In all cases, we find  $d_n \sim S \cdot s \cdot \lambda^{-n} \cdot \Gamma(n - \beta + 1)$ , where  $S, \lambda$  and  $\beta$  are the growth parameters of the corresponding anomalous dimension  $\gamma(\alpha)$ , eqs. (7.13), (8.2) and (9.3). This suggests that  $\delta(\alpha)$  receives non-perturbative contributions of the same type as does the anomalous dimension  $\gamma(\alpha)$  [11, 9]. The resemblance is particularly striking in the  $D = 4$  model, eq. (7.15).
- (5) Our numerical data suggests two new tentative exact results: The Stokes constant for  $s = -3$  in the  $D = 4$  model seems to be  $S(-3) = 3/(\pi e^2)$ , see section 7.2. And for the non-linear toy model at  $s = -2$  in MS, the anomalous dimension appears to be  $\bar{\gamma}(\alpha) = -\alpha$ . From this we deduced the exact non-perturbative Green function in both MOM and MS up to one integration constant, eqs. (9.4) and (9.5). However, this last result is not fully satisfactory since we can not clearly relate it to the perturbative formulation at the moment.

All examples indicate that there is a significant offset factor  $\delta(\alpha)$  between the mass scale  $\mu$  of MS-renormalization and the corresponding kinematic renormalization point. By eq. (3.11), the offset does not vanish in the limit of vanishing coupling. The tentative non-perturbative Green functions eqs. (9.4) and (9.5) show significantly different behaviour in MS versus MOM in the limit  $\alpha \rightarrow 0$ . Consequently one should be careful not to confuse the mass scale  $\mu$  of MS-renormalization with a kinematic renormalization point, even in the most well-behaved cases and even for “small coupling”.

For the linear DSEs, we have found an explicit map  $\gamma(\alpha) \mapsto \ln \delta(\alpha)$  in eqs. (4.15), (5.1) and (6.2). For the non-linear DSEs, this connection is not quite so simple. Intuitively, the identical asymptotic growth hints at the possibility to find an explicit map as well. Indeed, for the  $D = 4$  case, assuming that our empirical findings hold to all orders, eq. (7.15) reproduces the factorial growth of  $d_n$  and therefore the non-perturbative behaviour. The analytic remainder function  $f(\alpha)$  in this case remains to be identified.

## APPENDIX A. MELLIN TRANSFORMS

The Mellin transform is by definition the value of the primitive integral where one of the propagators is raised to a power  $1 + \rho$ , evaluated at unity external momentum. Factors of  $4\pi$  from the

Fourier transform are implicitly absorbed into the mass scale in the main text, therefore they are left out from the Mellin transform. For the 4-dimensional resp. 6-dimensional propagator,

$$M(\rho) = \int \frac{d^4k (k^2)^{-\rho}}{(k+q)^2 k^2} \Big|_{q^2=1} = \frac{1}{\rho(1-\rho)}, \quad M(\rho) = \int \frac{d^6k (k^2)^{-\rho}}{(k+q)^2 k^2} \Big|_{q^2=1} = -\frac{1}{\rho(1-\rho)(2-\rho)(3-\rho)}.$$

The Mellin transform in the toy model is

$$M(\rho) = \int_0^\infty \frac{dy y^{-\rho}}{x+y} \Big|_{x=1} = \frac{\pi}{\sin(\pi\rho)}.$$

## APPENDIX B. SERIES EXPANSION OF THE PRIMITIVE GRAPHS

We are interested in the series expansion in  $\epsilon$  of the integral

$$\begin{aligned} I_D^{(k)}(q) &:= \int \frac{d^D p}{(2\pi)^D} \frac{1}{(p+q)^2 (p^2)^{1+k\epsilon}} \\ &= (4\pi)^{-\frac{D}{2}} (q^2)^{\frac{D}{2}-2-k\epsilon} \frac{\Gamma(-\frac{D}{2}+2+k\epsilon) \Gamma(\frac{D}{2}-1) \Gamma(\frac{D}{2}-1-k\epsilon)}{\Gamma(1+k\epsilon) \Gamma(D-2-k\epsilon)} \\ &=: (4\pi)^{-\frac{D}{2}} (q^2)^{\frac{D}{2}-2-k\epsilon} e^{-\gamma_E \epsilon} \sum_n f_n^{(k)} \epsilon^n. \end{aligned}$$

The factors of  $q^2$  must not be expanded into logarithms, in order to be integrated in the next iteration. Furthermore, we do not expand the  $(4\pi)$  and factor out  $e^{-\gamma_E \epsilon}$  because both can conveniently be absorbed into the momentum. It remains to expand the gamma functions using

$$\Gamma(x+1) = x\Gamma(x), \quad \Gamma(1+\epsilon) = \exp\left(-\gamma_E \epsilon + \sum_{m=2}^{\infty} \frac{(-\epsilon)^m}{m} \zeta(m)\right).$$

In  $D = 4 - 2\epsilon$  dimensions one obtains

$$\begin{aligned} \Gamma &:= \frac{\Gamma((k+1)\epsilon)\Gamma(1-(k+1)\epsilon)\Gamma(1-\epsilon)}{\Gamma(1+k\epsilon)\Gamma(2-(k+2)\epsilon)} = \frac{1}{(k+1)(1-(k+2)\epsilon)\epsilon} \exp\left(-\gamma_E \epsilon + \sum_{m=2}^{\infty} T_m^{(k)} \epsilon^m\right), \\ \text{(B.1)} \quad \text{where} \quad T_m^{(k)} &:= (m-1)!((-1)^m(k+1)^m + (k+1)^m + 1 - (-k)^m - (k+2)^m) \zeta(m). \end{aligned}$$

Expanding the prefactor in a geometric series and leaving out  $e^{-\gamma_E \epsilon}$ ,

$$\text{(B.2)} \quad f_n^{(k)} = \sum_{t=-1}^n \frac{(k+2)^{t+1}}{k+1} \frac{1}{(n-t)!} \sum_{m=0}^{n-t} B_{n-t,m} \left(0, T_2^{(k)}, T_3^{(k)}, \dots, T_{n-t+1-m}^{(k)}\right).$$

Here  $B_{n,k}$  are incomplete Bell polynomials [4] [18, p 134]. For  $D = 6 - 2\epsilon$  dimensions, observe

$$\frac{\Gamma(-1+(k+1)\epsilon)\Gamma(2-\epsilon)\Gamma(2-(k+1)\epsilon)}{\Gamma(1+k\epsilon)\Gamma(4-(k+2)\epsilon)} = \frac{\epsilon-1}{(3-(k+2)\epsilon)(2-(k+2)\epsilon)} \cdot \Gamma.$$

The gamma functions on the right hand side are the same as in  $D = 4 - 2\epsilon$ , consequently their series expansion is again given by the polynomials  $T_m^{(k)}$  from eq. (B.1).

(B.3)

$$f_n^{(k)} = \sum_{t=-1}^n \left(-k+1 + \frac{k}{2^{t+1}} - \frac{k-1}{3^{t+2}}\right) \frac{(k+2)^t}{2(k+1)} \frac{1}{(n-t)!} \sum_{m=0}^{n-t} B_{n-t,m} \left(0, T_2^{(k)}, \dots, T_{n-t+1-m}^{(k)}\right).$$

In the toy model, the relevant integral and its series expansion are

$$\int_0^{\infty} \frac{dy y^{-(k+1)\epsilon}}{1+y} = \frac{\pi}{\sin(\pi(k+1)\epsilon)} = \Gamma((k+1)\epsilon)\Gamma(1-(k+1)\epsilon) =: \sum_{n=-1}^{\infty} f_n^{(k)} \epsilon^n.$$

The Bernoulli numbers  $B_n$  vanish when  $n > 1$  is odd, therefore we can write

$$(B.4) \quad f_n^{(k)} := \frac{1}{(k+1)} \sum_{m=0}^{n+1} \frac{1}{(n+1)!} B_{n+1,m} \left(0, T_2^{(k)}, \dots, T_{n+2-m}^{(k)}\right), \quad T_n^{(k)} := \left(2\pi(k+1)\right)^n \frac{|B_n|}{n}.$$

### APPENDIX C. KINEMATIC COUNTER TERM OF THE LINEAR TOY MODEL

These are the first coefficients of eq. (6.3) for the toy model. Define  $A := \alpha^2 \pi^2$ .

$$\begin{aligned} z_1 &= \frac{\alpha\pi^2(4+A)}{24(1-A)^{\frac{3}{2}}}, & z_2 &= \frac{\alpha^2\pi^4(3+2A)}{16(1-A)^3}, & z_3 &= \frac{\alpha\pi^4(112+2240A+2919A^2+254A^3)}{5760(1-A)^{\frac{9}{2}}}, \\ z_4 &= \frac{\alpha^2\pi^6(36+515A+900A^2+240A^3+4A^4)}{384(1-A)^6}, \\ z_5 &= \frac{\alpha\pi^6(1984+522152A+6074220A^2+12882535A^3+6095260A^4+511956A^5+1768A^6)}{967680(1-A)^{\frac{15}{2}}}, \\ z_6 &= \frac{\alpha^2\pi^8(471+42058A+428661A^2+1041030A^3+715270A^4+129414A^5+4092A^6+4A^7)}{11520(1-A)^9}. \end{aligned}$$

All explicitly determined functions  $z_n(\alpha)$  for  $n > 0$  behave qualitatively similar: They diverge like  $(1-A)^{-\frac{3}{2}n}$  as  $\alpha\pi \rightarrow 1$  and are positive for  $0 \leq \alpha < \frac{1}{\pi}$ . In this interval, they give rise to a finite  $Z$ -factor. The other coefficients in eq. (6.3) are

$$\begin{aligned} z'_1 &= \frac{1}{\epsilon} + \frac{\pi^2}{6}\epsilon + \frac{7\pi^4}{360}\epsilon^3 + \dots = -\frac{1}{\epsilon} \sum_{n=0}^{\infty} \frac{(-1)^n(4^n-2)B_{2n}}{(2n)!} \pi^{2n} \epsilon^{2n} = \pi \left( \cot\left(\frac{\pi}{2}\epsilon\right) - \cot(\pi\epsilon) \right), \\ z'_2 &= \frac{\pi^2}{4} \frac{1}{\cos^2\left(\frac{\pi}{2}\epsilon\right) \cos(\pi\epsilon)}, & z'_3 &= \frac{\pi^3}{12} \frac{1-2\cos(2\pi\epsilon)+2\cos(\pi\epsilon)}{(2\cos(\pi\epsilon)+3\cos(3\pi\epsilon)) \sin\left(\frac{\pi}{2}\epsilon\right) \cos^3\left(\frac{\pi}{2}\epsilon\right)}, \\ z'_4 &= -\frac{\pi^4}{4} \frac{\cos(\pi\epsilon)+2\sin^2(\pi\epsilon)}{\cos^4(\pi\epsilon)(\cos(\pi\epsilon)-4\cos^2(\pi\epsilon)\cos(2\pi\epsilon)+\cos(3\pi\epsilon))}. \end{aligned}$$

The functions  $z'_n(\epsilon)$  are positive for small positive  $\epsilon$ . They change sign at their poles but probably, there are other continuations of the series expansion around  $\epsilon = 0$  beyond the poles, which stay positive. For example

$$z'_2(\epsilon) = \frac{\pi^2}{2} \left( \frac{1}{\sin^2(\pi\epsilon)} - \frac{|\cot(\pi\epsilon) - \cot\left(\frac{\pi}{2}\epsilon\right)|^3}{|\cot(\pi\epsilon)|} \right)$$

is always positive and reduces to the above form of  $z'_2$  for  $|\epsilon| < 0.5$ . If this holds for all  $z'_n$  then  $Z(\alpha, \epsilon) \in [0, 1]$ , which allows to interpret  $Z$  as a probability.

APPENDIX D. ASYMPTOTIC GROWTH OF THE ANOMALOUS DIMENSION

For the 4-dimensional physical model, the ansatz eq. (7.8) delivers the growth parameters

$$(D.1) \quad \lambda = \frac{1}{s}, \quad \beta(s) = -\frac{3+2s}{s}, \quad b^{(1)}(s) = -\frac{1+4s+3s^2}{s}, \quad b^{(2)}(s) = \frac{1+6s+8s^2-2s^3-5s^4}{2s^2}$$

$$b^{(3)}(s) = \frac{-1-6s-s^2+24s^3-25s^4-126s^5-81s^6}{6s^3}.$$

They match [11, (14)] for  $s = -2$ . For the 6-dimensional physical model, there are three solutions:

$$(D.2) \quad \vec{\lambda}(s) = \left( -\frac{6}{s}, -\frac{12}{s}, -\frac{18}{s} \right), \quad \vec{\beta}(s) = \left( -\frac{35+29s}{6s}, -\frac{5+2s}{3s}, -\frac{15+13s}{2s} \right)$$

$$\vec{b}^{(1)}(s) = \left( \frac{-275-267s+8s^2}{216s}, \frac{265+624s+359s^2}{108s}, \frac{85+241s+156s^2}{72s} \right)$$

$$\vec{b}^{(2)}(s) = \left( \frac{75625+83790s-101849s^2-177828s^3-67814s^4}{93312s^2}, \frac{70225+339690s+602764s^2+465258s^3+131959s^4}{23328s^2}, \frac{7225+37950s+69779s^2+51628s^3+12574s^4}{10368s^2} \right)$$

$$\vec{b}^{(3)}(s) = \left( \frac{-20796875-8551125s+107422197s^2+206297091s^3+177713418s^4+90251478s^5+23658704s^6}{60466176s^3}, \frac{18609625+138592350s+424432473s^2+687305592s^3+624311121s^4+303609366s^5+62154089s^6}{7558272s^3}, \frac{614125+4453575s+12499453s^2+16989843s^3+11830354s^4+4259034s^5+758520s^6}{2239488s^3} \right)$$

Including order  $1/n^3$ , the large-order growth of  $c_n$  is determined entirely by the first component of these vectors. In order to match [9, eqs. (41)-(43)],  $b^{(1)}$  has to be multiplied with 3,  $b^{(2)}$  with 9 and  $b^{(3)}$  with 27. Parameters for the toy model are given in table 11.

APPENDIX E. TABLES

| $s$ | $\gamma(\alpha)$  |
|-----|---|
| 5   | $-\alpha - 6\alpha^2 - 102\alpha^3 - 2640\alpha^4 - 87804\alpha^5 - 3483072\alpha^6 - 158329512\alpha^7 - 8050087584\alpha^8$ |
| 4   | $-\alpha - 5\alpha^2 - 70\alpha^3 - 1485\alpha^4 - 40370\alpha^5 - 1306370\alpha^6 - 48365100\alpha^7 - 2000065725\alpha^8$   |
| 3   | $-\alpha - 4\alpha^2 - 44\alpha^3 - 728\alpha^4 - 15368\alpha^5 - 384960\alpha^6 - 11004672\alpha^7 - 350628096\alpha^8$      |
| 2   | $-\alpha - 3\alpha^2 - 24\alpha^3 - 285\alpha^4 - 4284\alpha^5 - 75978\alpha^6 - 1530720\alpha^7 - 34237485\alpha^8$          |
| 1   | $-\alpha - 2\alpha^2 - 10\alpha^3 - 72\alpha^4 - 644\alpha^5 - 6704\alpha^6 - 78408\alpha^7 - 1008480\alpha^8$                |
| 0   | $-\alpha - \alpha^2 - 2\alpha^3 - 5\alpha^4 - 14\alpha^5 - 42\alpha^6 - 132\alpha^7 - 429\alpha^8$                            |
| -1  | $-\alpha$   |
| -2  | $-\alpha + \alpha^2 - 4\alpha^3 + 27\alpha^4 - 248\alpha^5 + 2830\alpha^6 - 38232\alpha^7 + 593859\alpha^8$                   |
| -3  | $-\alpha + 2\alpha^2 - 14\alpha^3 + 160\alpha^4 - 2444\alpha^5 + 45792\alpha^6 - 1005480\alpha^7 + 25169760\alpha^8$          |
| -4  | $-\alpha + 3\alpha^2 - 30\alpha^3 + 483\alpha^4 - 10314\alpha^5 + 268686\alpha^6 - 8167068\alpha^7 + 281975715\alpha^8$       |
| -5  | $-\alpha + 4\alpha^2 - 52\alpha^3 + 1080\alpha^4 - 29624\alpha^5 + 988288\alpha^6 - 38377152\alpha^7 + 1689250176\alpha^8$    |

TABLE 6. Non-linear DSE in  $D = 4$  dimensions, see section 7.2. Series expansion of the anomalous dimension in MOM as a function of the renormalized coupling  $\alpha$  up to order  $\alpha^8$  for various powers  $s$  of the invariant charge  $Q = G^s$ . Only insertions into a single internal edge were performed in all cases.

| $s$ | $S(s)$   |
|-----|--|
| 5   | -0.025 296 711 447 842 155 554 062 589 810 922 604 262 477 942 805 771   |
| 4   | -0.027 093 755 285 804 302 538 145 834 438 779 321 901 953 254 099 492   |
| 3   | -0.027 514 268 695 235 967 509 951 466 619 196 206 136 028 416 088 749   |
| 2   | -0.022 754 314 527 304 604 570 864 961 094 569 471 756 231 077 114 904   |
| 1   | -0.005 428 317 993 266 202 636 748 034 138 132 075 286 101 589 263 688 3 |
| -2  | 0.207 553 748 710 297 351 670 134 124 720 668 682 684 453 514 969 63     |
| -3  | 0.129 235 675 811 091 778 715 229 366 859 663 994 914 292 887 084 30     |
| -4  | 0.087 977 369 959 821 254 076 048 394 021 324 447 743 442 962 588 612    |
| -5  | 0.065 314 016 354 658 749 144 010 387 750 377 100 215 558 556 707 446    |

TABLE 7. First 50 digits of the Stokes constant  $S(s)$  for the non-linear DSE in  $D = 4$ , see eq. (7.9). One finds  $S(-2) = (\sqrt{\pi}e)^{-1}$  and  $S(-3) = 3(\sqrt{\pi}e)^{-2}$

| $s$ | $\ln \bar{\delta}(\alpha)$  | $f_{n+1}/f_n$    |
|-----|---|------------------|
| 5   | $-2 - 9\alpha + (-139 + 14\zeta(3))\alpha^2 + \left(-3464 - \frac{7\pi^4}{12} + 233\zeta(3)\right)\alpha^3$   | $30.22 \pm 0.09$ |
| 4   | $-2 - \frac{15}{2}\alpha + \left(-\frac{575}{6} + 10\zeta(3)\right)\alpha^2 + \left(-\frac{23525}{12} - \frac{\pi^4}{3} + \frac{410}{3}\zeta(3)\right)\alpha^3$ | $25.09 \pm 0.06$ |
| 3   | $-2 - 6\alpha + \left(-\frac{182}{3} + \frac{20}{3}\zeta(3)\right)\alpha^2 + \left(-\frac{2911}{3} - \frac{\pi^4}{6} + \frac{214}{3}\zeta(3)\right)\alpha^3$    | $19.96 \pm 0.04$ |
| 2   | $-2 - \frac{9}{2}\alpha + \left(-\frac{67}{2} + 4\zeta(3)\right)\alpha^2 + \left(-\frac{773}{2} - \frac{\pi^4}{15} + 31\zeta(3)\right)\alpha^3$                 | $14.80 \pm 0.02$ |
| 1   | $-2 - 3\alpha + \left(-\frac{43}{3} + 2\zeta(3)\right)\alpha^2 + \left(-\frac{305}{3} - \frac{\pi^4}{60} + \frac{29}{3}\zeta(3)\right)\alpha^3$                 | $9.60 \pm 0.01$  |
| 0   | $-2 - \frac{3}{2}\alpha + \left(-\frac{19}{6} + \frac{2}{3}\zeta(3)\right)\alpha^2 + \left(-\frac{103}{12} + \frac{4}{3}\zeta(3)\right)\alpha^3$                |                  |
| -1  | -2  |                  |
| -2  | $-2 + \frac{3}{2}\alpha - \frac{29}{6}\alpha^2 + \left(\frac{94}{3} - \frac{1}{3}\zeta(3)\right)\alpha^3$   | $5.8 \pm 1.8$    |
| -3  | $-2 + 3\alpha + \left(-\frac{53}{3} + \frac{2}{3}\zeta(3)\right)\alpha^2 + \left(\frac{578}{3} + \frac{\pi^4}{60} - \frac{17}{3}\zeta(3)\right)\alpha^3$        | $10.50 \pm 0.11$ |
| -4  | $-2 + \frac{9}{2}\alpha + \left(-\frac{77}{2} + 2\zeta(3)\right)\alpha^2 + \left(\frac{2365}{4} + \frac{\pi^4}{15} - 22\zeta(3)\right)\alpha^3$                 | $15.69 \pm 0.05$ |
| -5  | $-2 + 6\alpha + \left(-\frac{202}{3} + 4\zeta(3)\right)\alpha^2 + \left(\frac{4003}{3} + \frac{\pi^4}{6} - \frac{166}{3}\zeta(3)\right)\alpha^3$                | $20.85 \pm 0.07$ |

TABLE 8. Non-linear DSE in  $D = 4$  dimensions.  $\ln \bar{\delta}(\alpha)$  is the logarithm of the shift in the renormalization point between MOM- and MS-scheme eq. (3.2). Shown are the first terms of its perturbative power series.  $f_{n+1}/f_n$  is the growth rate of the function  $f(\alpha)$  in eq. (7.15).

| $s$ | $10^6 \cdot S(s)$  |
|-----|--|
| 5   | -48.879 979 612 936 267 148 575 174 247 043 686 402 701 421 680 529      |
| 4   | -33.683 126 435 179 258 367 949 154 667 346 857 343 063 662 040 223      |
| 3   | -16.197 057 487 106 552 084 835 982 615 789 341 267 879 644 562 145      |
| 2   | -2.874 931 066 358 404 169 842 007 765 677 311 801 515 635 631 211 6     |
| 1   | -0.005 037 643 852 252 104 613 165 864 641 040 152 093 341 435 216 537 2 |
| -2  | 87 595.552 909 179 124 483 795 447 421 262 990 627 388 017 406 822       |
| -3  | 17 853.256 793 175 269 493 347 991 077 950 813 245 133 374 820 922       |
| -4  | 6637.593 110 037 931 650 951 894 178 458 603 722 595 701 766 465 0       |
| -5  | 3384.186 761 682 513 227 965 148 628 942 508 807 465 013 504 317 6       |

TABLE 9. First 50 digits of the Stokes constant  $S(s)$  for  $D = 6$ , see eq. (7.9).

| $s$ | $\ln \delta(\alpha)$  |
|-----|---|
| 5   | $-\frac{8}{3} + \frac{61}{24}\alpha + \left(-\frac{80213}{7776} + \frac{7}{18}\zeta(3)\right)\alpha^2 + \left(\frac{8813575}{139968} + \frac{7\pi^4}{2592} - \frac{2563}{1296}\zeta(3)\right)\alpha^3$      |
| 4   | $-\frac{8}{3} + \frac{305}{144}\alpha + \left(-\frac{331345}{46656} + \frac{5}{18}\zeta(3)\right)\alpha^2 + \left(\frac{119812205}{3359232} + \frac{\pi^4}{648} - \frac{2255}{1944}\zeta(3)\right)\alpha^3$ |
| 3   | $-\frac{8}{3} + \frac{61}{36}\alpha + \left(-\frac{52325}{11664} + \frac{5}{27}\zeta(3)\right)\alpha^2 + \left(\frac{14842891}{839808} + \frac{\pi^4}{1296} - \frac{1177}{1944}\zeta(3)\right)\alpha^3$     |
| 2   | $-\frac{8}{3} + \frac{61}{48}\alpha + \left(-\frac{38381}{15552} + \frac{1}{9}\zeta(3)\right)\alpha^2 + \left(\frac{3947825}{559872} + \frac{\pi^4}{3240} - \frac{341}{1296}\zeta(3)\right)\alpha^3$        |
| 1   | $-\frac{8}{3} + \frac{61}{72}\alpha + \left(-\frac{24437}{23328} + \frac{1}{18}\zeta(3)\right)\alpha^2 + \left(\frac{1560359}{839808} + \frac{\pi^4}{12960} - \frac{319}{3888}\zeta(3)\right)\alpha^3$      |
| 0   | $-\frac{8}{3} + \frac{61}{144}\alpha + \left(-\frac{10493}{46656} + \frac{1}{54}\zeta(3)\right)\alpha^2 + \left(\frac{518095}{3359232} - \frac{11}{972}\zeta(3)\right)\alpha^3$                             |
| -1  | $-\frac{8}{3}$  |
| -2  | $-\frac{8}{3} - \frac{61}{144}\alpha - \frac{17395}{46656}\alpha^2 + \left(-\frac{114361}{209952} + \frac{11}{3888}\zeta(3)\right)\alpha^3$   |
| -3  | $-\frac{8}{3} - \frac{61}{72}\alpha + \left(\frac{31339}{23328} + \frac{1}{54}\zeta(3)\right)\alpha^2 + \left(-\frac{359005}{104976} - \frac{\pi^4}{12960} + \frac{187}{3888}\zeta(3)\right)\alpha^3$       |
| -4  | $-\frac{8}{3} - \frac{61}{48}\alpha + \left(-\frac{45283}{15552} + \frac{1}{18}\zeta(3)\right)\alpha^2 + \left(-\frac{11830593}{1119744} - \frac{\pi^4}{3240} + \frac{121}{648}\zeta(3)\right)\alpha^3$     |
| -5  | $-\frac{8}{3} - \frac{61}{36}\alpha + \left(-\frac{59227}{11664} + \frac{1}{9}\zeta(3)\right)\alpha^2 + \left(-\frac{20089615}{839808} - \frac{\pi^4}{1296} + \frac{913}{1944}\zeta(3)\right)\alpha^3$      |

TABLE 10. First perturbative coefficients of  $\ln \delta(\alpha)$  for  $D = 6$  dimensions.

| $s$ | $S(s)$                        | $b^{(1)}(s)$                | $b^{(2)}(s)$         |
|-----|-------------------------------|-----------------------------|----------------------|
| 5   | -0.323 584 398 140 310 305 46 | -33.713 129 682 396 588 961 | 565.374 787 298 670  |
| 4   | -0.391 335 083 719 234 905 86 | -28.505 508 252 042 547 410 | 405.630 022 359 080  |
| 3   | -0.488 736 158 026 247 795 99 | -23.352 717 957 250 113 407 | 273.573 399 332 400  |
| 2   | -0.620 736 529 443 448 896 58 | -18.337 005 501 361 698 274 | 169.862 094 180 663  |
| 1   | -0.595 434 011 519 108 439 04 | -13.869 604 401 089 358 619 | 98.052 567 522 448 0 |
| -2  | 0.636 619 772 367 581 343 08  | 4.467 401 100 272 339 654 7 | 7.978 836 295 357 26 |
| -3  | 0.526 186 295 467 803 784 50  | 9.483 113 556 160 754 788 2 | 40.254 589 493 216 4 |
| -4  | 0.419 256 495 256 609 057 56  | 14.635 903 850 953 188 791  | 98.974 445 168 262 5 |
| -5  | 0.343 587 215 470 932 442 58  | 19.843 525 281 307 230 343  | 184.621 956 597 118  |

TABLE 11. First digits of the Stokes constant  $S(s)$  and subleading corrections of the asymptotic growth eq. (7.9) of the anomalous dimension in the toy model section 9.

| $s$ | $\alpha \ln \delta(\alpha(A))$  |
|-----|---|
| 5   | $-6A - \frac{2009}{3}A^2 - \frac{11563106}{45}A^3 - \frac{173306477104}{945}A^4 - \frac{1228737945883358}{6075}A^5 - \frac{46235332362117842849}{147015}A^6$  |
| 4   | $-5A - \frac{1130}{3}A^2 - \frac{4316822}{45}A^3 - \frac{59632972484}{1323}A^4 - \frac{461687074578658}{14175}A^5 - \frac{34025588969113725668}{1029105}A^6$  |
| 3   | $-4A - \frac{554}{3}A^2 - \frac{1263424}{45}A^3 - \frac{10282878575}{1323}A^4 - \frac{46540947260036}{14175}A^5 - \frac{398737839692532122}{205821}A^6$       |
| 2   | $-3A - \frac{217}{3}A^2 - \frac{1233338}{225}A^3 - \frac{4881119933}{6615}A^4 - \frac{3528108924854}{23625}A^5 - \frac{1074400592111547046}{25727625}A^6$     |
| 1   | $-2A - \frac{55}{3}A^2 - \frac{106898}{225}A^3 - \frac{135875429}{6615}A^4 - \frac{272890120256}{212625}A^5 - \frac{2770658834393158}{25727625}A^6$           |
| 0   | $-A - \frac{4}{3}A^2 - \frac{146}{45}A^3 - \frac{8864}{945}A^4 - \frac{417682}{14175}A^5 - \frac{9095176}{93555}A^6$  |
| -1  | 0   |
| -2  | $A + 7A^2 + 242A^3 + 17771A^4 + 2189294A^5 + 404590470A^6$  |
| -3  | $2A + 41A^2 + \frac{92518}{25}A^3 + \frac{503885698}{735}A^4 + \frac{1639676026462}{7875}A^5 + \frac{266517331818761291}{2858625}A^6$                         |
| -4  | $3A + \frac{370}{3}A^2 + \frac{4782122}{225}A^3 + \frac{48904622516}{6615}A^4 + \frac{887103429351554}{212625}A^5 + \frac{88600913717695595572}{25727625}A^6$ |
| -5  | $4A + \frac{826}{3}A^2 + \frac{3478864}{45}A^3 + \frac{287007344207}{6615}A^4 + \frac{185545372999796}{4725}A^5 + \frac{53252838327756373006}{1029105}A^6$    |

TABLE 12. First coefficients of  $\ln \delta(\alpha)$  in the toy model section 9, up to order  $\alpha^{11}$ . Here,  $A := (\alpha\pi)^2/4$ .

## REFERENCES

- [1] G. 't Hooft. “Dimensional Regularization and the Renormalization Group”. In: *Nuclear Physics B* 61 (Sept. 24, 1973), pp. 455–468. ISSN: 0550-3213. DOI: 10.1016/0550-3213(73)90376-3. URL: <https://www.sciencedirect.com/science/article/pii/0550321373903763>.
- [2] G. 't Hooft and M. Veltman. “Regularization and Renormalization of Gauge Fields”. In: *Nuclear Physics B* 44.1 (July 1, 1972), pp. 189–213. ISSN: 0550-3213. DOI: 10.1016/0550-3213(72)90279-9. URL: <http://www.sciencedirect.com/science/article/pii/0550321372902799>.
- [3] Inês Aniceto, Gökçe Başar, and Ricardo Schiappa. “A Primer on Resurgent Transseries and Their Asymptotics”. In: *Physics Reports. A Primer on Resurgent Transseries and Their Asymptotics* 809 (May 25, 2019), pp. 1–135. ISSN: 0370-1573. DOI: 10.1016/j.physrep.2019.02.003. URL: <https://www.sciencedirect.com/science/article/pii/S0370157319300730>.
- [4] E. T. Bell. “Exponential Polynomials”. In: *Annals of Mathematics* 35.2 (1934), pp. 258–277. ISSN: 0003-486X. DOI: 10.2307/1968431. JSTOR: 1968431.
- [5] Marc Bellon. “An Efficient Method for the Solution of Schwinger–Dyson Equations for Propagators”. In: *Letters in Mathematical Physics* 94.1 (Oct. 2010), pp. 77–86. ISSN: 0377-9017, 1573-0530. DOI: 10.1007/s11005-010-0415-3. arXiv: 1005.0196. URL: <http://arxiv.org/abs/1005.0196>.
- [6] Marc Bellon and Fidel A. Schaposnik. “Renormalization Group Functions for the Wess-Zumino Model: Up to 200 Loops through Hopf Algebras”. In: *Nuclear Physics B* 800.3 (Sept. 2008), pp. 517–526. ISSN: 05503213. DOI: 10.1016/j.nuclphysb.2008.02.005. arXiv: 0801.0727. URL: <http://arxiv.org/abs/0801.0727>.
- [7] Marc P. Bellon. “Approximate Differential Equations for Renormalization Group Functions in Models Free of Vertex Divergencies”. In: *Nuclear Physics B* 826.3 (Feb. 21, 2010), pp. 522–531. ISSN: 0550-3213. DOI: 10.1016/j.nuclphysb.2009.11.002. URL: <https://www.sciencedirect.com/science/article/pii/S0550321309005896>.
- [8] C. G. Bollini and J. J. Giambiagi. “Dimensional Renormalization : The Number of Dimensions as a Regularizing Parameter”. In: *Il Nuovo Cimento B (1971-1996)* 12.1 (Nov. 1, 1972), pp. 20–26. ISSN: 1826-9877. DOI: 10.1007/BF02895558. URL: <https://doi.org/10.1007/BF02895558>.
- [9] M. Borinsky, G. Dunne, and Max Meynig. “Semiclassical Trans-Series from the Perturbative Hopf-Algebraic Dyson-Schwinger Equations:  $\phi^3$  QFT in 6 Dimensions”. In: *Symmetry, Integrability and Geometry: Methods and Applications* 17 (2021), pp. 87–113. DOI: 10.3842/SIGMA.2021.087. URL: <https://doi.org/10.3842/SIGMA.2021.087>.
- [10] Michael Borinsky. *Generating Asymptotics for Factorially Divergent Sequences*. Version 4. Oct. 8, 2018. arXiv: 1603.01236 [math-ph]. URL: <http://arxiv.org/abs/1603.01236>.
- [11] Michael Borinsky and Gerald V. Dunne. “Non-Perturbative Completion of Hopf-algebraic Dyson-Schwinger Equations”. In: *Nuclear Physics B* 957 (Aug. 1, 2020), p. 115096. ISSN: 0550-3213. DOI: 10.1016/j.nuclphysb.2020.115096. URL: <http://www.sciencedirect.com/science/article/pii/S0550321320301826>.
- [12] D. J. Broadhurst and D. Kreimer. “Combinatoric Explosion of Renormalization Tamed by Hopf Algebra: 30-Loop Pade-Borel Resummation”. In: *Physics Letters B* 475.1-2 (Feb. 2000), pp. 63–70. ISSN: 03702693. DOI: 10.1016/S0370-2693(00)00051-4. arXiv: hep-th/9912093. URL: <http://arxiv.org/abs/hep-th/9912093>.
- [13] D. J. Broadhurst and D. Kreimer. “Exact Solutions of Dyson-Schwinger Equations for Iterated One-Loop Integrals and Propagator-Coupling Duality”. In: *Nuclear Physics B* 600.2 (Apr. 2001), pp. 403–422. ISSN: 05503213. DOI: 10.1016/S0550-3213(01)00071-2. arXiv: hep-th/0012146. URL: <http://arxiv.org/abs/hep-th/0012146>.

- [14] Francis Brown and Dirk Kreimer. *Angles, Scales and Parametric Renormalization*. Dec. 6, 2011. arXiv: 1112.1180 [hep-th]. URL: <http://arxiv.org/abs/1112.1180>.
- [15] Curtis G. Callan. “Broken Scale Invariance in Scalar Field Theory”. In: *Physical Review D* 2.8 (Oct. 15, 1970), pp. 1541–1547. DOI: 10.1103/PhysRevD.2.1541. URL: <https://link.aps.org/doi/10.1103/PhysRevD.2.1541>.
- [16] William Celmaster and Richard J. Gonsalves. “Renormalization-Prescription Dependence of the Quantum-Chromodynamic Coupling Constant”. In: *Physical Review D* 20.6 (Sept. 15, 1979), pp. 1420–1434. DOI: 10.1103/PhysRevD.20.1420. URL: <https://link.aps.org/doi/10.1103/PhysRevD.20.1420>.
- [17] J. C. Collins and A. J. Macfarlane. “New Methods for the Renormalization Group”. In: *Physical Review D* 10.4 (Aug. 15, 1974), pp. 1201–1212. DOI: 10.1103/PhysRevD.10.1201. URL: <https://link.aps.org/doi/10.1103/PhysRevD.10.1201>.
- [18] Louis Comtet. *Advanced Combinatorics*. Dordrecht, Holland: D. Reidel Publishing Company, 1974. ISBN: 978-94-010-2198-2.
- [19] Alain Connes and Dirk Kreimer. “Renormalization in Quantum Field Theory and the Riemann-Hilbert Problem II: The Beta-Function, Diffeomorphisms and the Renormalization Group”. In: *Communications in Mathematical Physics* 216.1 (Jan. 2001), pp. 215–241. ISSN: 0010-3616. DOI: 10.1007/PL00005547. arXiv: hep-th/0003188. URL: <http://arxiv.org/abs/hep-th/0003188>.
- [20] Alain Connes and Matilde Marcolli. *Noncommutative Geometry, Quantum Fields and Motives*. Vol. 55. Colloquium Publications. Providence, Rhode Island: American Mathematical Society, Dec. 20, 2007. ISBN: 978-0-8218-4210-2 978-1-4704-3201-0. DOI: 10.1090/coll/055. URL: <http://www.ams.org/coll/055>.
- [21] Julien Courtiel and Karen Yeats. “Next-to-k Leading Log Expansions by Chord Diagrams”. In: *Communications in Mathematical Physics* 377.1 (July 1, 2020), pp. 469–501. ISSN: 1432-0916. DOI: 10.1007/s00220-020-03691-7. URL: <https://doi.org/10.1007/s00220-020-03691-7>.
- [22] R. Delbourgo, D. Elliott, and D. S. McAnally. “Dimensional Renormalization in Phi3 Theory: Ladders and Rainbows”. In: *Physical Review D* 55.8 (Apr. 15, 1997), pp. 5230–5233. DOI: 10.1103/PhysRevD.55.5230. URL: <https://link.aps.org/doi/10.1103/PhysRevD.55.5230>.
- [23] R. Delbourgo, A. C. Kalloniatis, and G. Thompson. “Dimensional Renormalization: Ladders and Rainbows”. In: *Physical Review D* 54.8 (Oct. 15, 1996), pp. 5373–5376. DOI: 10.1103/PhysRevD.54.5373. URL: <https://link.aps.org/doi/10.1103/PhysRevD.54.5373>.
- [24] F. J. Dyson. “The S Matrix in Quantum Electrodynamics”. In: *Physical Review* 75.11 (June 1, 1949), pp. 1736–1755. DOI: 10.1103/PhysRev.75.1736. URL: <https://link.aps.org/doi/10.1103/PhysRev.75.1736>.
- [25] David J. Gross. “Applications of the Renormalization Group to High-Energy Physics”. In: *Methods in Field Theory, Les Houches Session 1975*. Ed. by Roger Balian and Jean Zinn-Justin. Les Houches Session 28. North Holland / World Scientific, 1981, pp. 141–250. ISBN: 978-9971-83-078-7. URL: <https://doi.org/10.1142/0004>.
- [26] Henry Kißler. “Systems of Linear Dyson–Schwinger Equations”. In: *Mathematical Physics, Analysis and Geometry* 22.3 (Aug. 29, 2019), p. 20. ISSN: 1572-9656. DOI: 10.1007/s11040-019-9320-x. URL: <https://doi.org/10.1007/s11040-019-9320-x>.
- [27] Lutz Klaczynski. *Haag’s Theorem in Renormalised Quantum Field Theories*. Feb. 1, 2016. arXiv: 1602.00662 [hep-th, physics:math-ph]. URL: <http://arxiv.org/abs/1602.00662>.
- [28] Lutz Klaczynski. “Resurgent Transseries  $\&\&$  Dyson-Schwinger Equations”. In: *Annals of Physics* 372 (Sept. 2016), pp. 397–448. ISSN: 00034916. DOI: 10.1016/j.aop.2016.06.003. arXiv: 1601.04140. URL: <http://arxiv.org/abs/1601.04140>.

- [29] Dirk Kreimer. “Étude for Linear Dyson–Schwinger Equations”. In: *Traces in Number Theory, Geometry and Quantum Fields*. Aspects of Mathematics E38. Wiesbaden: Friedr. Vieweg, 2008, pp. 155–160. URL: <http://preprints.ihes.fr/2006/P/P-06-23.pdf>.
- [30] Dirk Kreimer and Karen Yeats. “An Etude in Non-Linear Dyson–Schwinger Equations”. In: *Nuclear Physics B - Proceedings Supplements*. Proceedings of the 8th DESY Workshop on Elementary Particle Theory 160 (Oct. 1, 2006), pp. 116–121. ISSN: 0920-5632. DOI: 10.1016/j.nuclphysbps.2006.09.036. URL: <http://www.sciencedirect.com/science/article/pii/S0920563206006347>.
- [31] Olaf Krüger. “Log Expansions from Combinatorial Dyson–Schwinger Equations”. In: *Letters in Mathematical Physics* 110.8 (Aug. 1, 2020), pp. 2175–2202. ISSN: 1573-0530. DOI: 10.1007/s11005-020-01288-8. URL: <https://doi.org/10.1007/s11005-020-01288-8>.
- [32] Olaf Krüger and Dirk Kreimer. “Filtrations in Dyson–Schwinger Equations: Next-to-j-leading Log Expansions Systematically”. In: *Annals of Physics* 360 (Sept. 1, 2015), pp. 293–340. ISSN: 0003-4916. DOI: 10.1016/j.aop.2015.05.013. URL: <https://www.sciencedirect.com/science/article/pii/S0003491615001979>.
- [33] G. Mack and I. T. Todorov. “Conformal-Invariant Green Functions Without Ultraviolet Divergences”. In: *Physical Review D* 8.6 (Sept. 15, 1973), pp. 1764–1787. DOI: 10.1103/PhysRevD.8.1764. URL: <https://link.aps.org/doi/10.1103/PhysRevD.8.1764>.
- [34] Alan J. McKane. “Perturbation Expansions at Large Order: Results for Scalar Field Theories Revisited”. In: *Journal of Physics A: Mathematical and Theoretical* 52.5 (Feb. 1, 2019), p. 055401. ISSN: 1751-8113, 1751-8121. DOI: 10.1088/1751-8121/aaf768. arXiv: 1807.00656. URL: <http://arxiv.org/abs/1807.00656>.
- [35] Erik Panzer. *Hopf Algebraic Renormalization of Kreimer’s Toy Model*. Feb. 16, 2012. arXiv: 1202.3552 [hep-th, physics:math-ph]. URL: <http://arxiv.org/abs/1202.3552>.
- [36] Lewis Fry Richardson and Richard Tetley Glazebrook. “IX. The Approximate Arithmetical Solution by Finite Differences of Physical Problems Involving Differential Equations, with an Application to the Stresses in a Masonry Dam”. In: *Philosophical Transactions of the Royal Society of London. Series A, Containing Papers of a Mathematical or Physical Character* 210.459-470 (Jan. 1, 1911), pp. 307–357. DOI: 10.1098/rsta.1911.0009. URL: <https://royalsocietypublishing.org/doi/10.1098/rsta.1911.0009>.
- [37] Julian Schwinger. “On the Green’s Functions of Quantized Fields. II”. In: *Proceedings of the National Academy of Sciences* 37.7 (July 1, 1951), pp. 455–459. ISSN: 0027-8424, 1091-6490. DOI: 10.1073/pnas.37.7.455. pmid: 16578384. URL: <https://www.pnas.org/content/37/7/455>.
- [38] N. J. A. Sloane (editor). *The On-Line Encyclopedia of Integer Sequences*. 2018. URL: <https://oeis.org>.
- [39] K. Symanzik. “Small Distance Behaviour in Field Theory and Power Counting”. In: *Communications in Mathematical Physics* 18.3 (Sept. 1, 1970), pp. 227–246. ISSN: 1432-0916. DOI: 10.1007/BF01649434. URL: <https://doi.org/10.1007/BF01649434>.
- [40] Karen Yeats. *Growth Estimates for Dyson-Schwinger Equations*. Oct. 13, 2008. arXiv: 0810.2249 [math-ph]. URL: <http://arxiv.org/abs/0810.2249>.